
Simple and Effective Masked Diffusion Language Models

Subham Sekhar Sahoo
Cornell Tech, NYC, USA.
ssahoo@cs.cornell.edu

Marianne Arriola
Cornell Tech, NYC, USA.
ma2238@cornell.edu

Yair Schiff
Cornell Tech, NYC, USA.
yzs2@cornell.edu

Aaron Gokaslan
Cornell Tech, NYC, USA.
akg87@cs.cornell.edu

Edgar Marroquin
Cornell Tech, NYC, USA.
emm392@cornell.edu

Justin T Chiu
Cornell Tech, NYC, USA.
jtc257@cornell.edu

Alexander Rush
Cornell Tech, NYC, USA.
ar459@cornell.edu

Volodymyr Kuleshov
Cornell Tech, NYC, USA.
kuleshov@cornell.edu

Abstract

While diffusion models excel at generating high-quality images, prior work reports a significant performance gap between diffusion and autoregressive (AR) methods in language modeling. In this work, we show that simple masked discrete diffusion is more performant than previously thought. We apply an effective training recipe that improves the performance of masked diffusion models and derive a simplified, Rao-Blackwellized objective that results in additional improvements. Our objective has a simple form—it is a mixture of classical masked language modeling losses—and can be used to train encoder-only language models that admit efficient samplers, including ones that can generate arbitrary lengths of text semi-autoregressively like a traditional language model. On language modeling benchmarks, a range of masked diffusion models trained with modern engineering practices achieves a new state-of-the-art among diffusion models, and approaches AR perplexity. We release our code at: <https://github.com/kuleshov-group/mdlm>

1 Introduction

Diffusion models excel at producing realistic, high-quality images and have received significant attention as potential tools for generating discrete data such as text [1, 23, 25], biological sequences [2], and graphs [45, 48]. Unlike autoregressive (AR) approaches, diffusion-based methods are not constrained to generate data sequentially, and therefore have the potential to improve long-term planning, controllable generation, and sampling speed. However, discrete diffusion methods exhibit a performance gap relative to AR models [1, 17, 19, 25], especially in language modeling. The standard measure of language modeling performance is log-likelihood: when controlling for parameter count, prior work reports a sizable log-likelihood gap between AR and diffusion models.

In this work, we show that simple masked diffusion language modeling (MDLM) combined with effective training recipes is more performant than previously thought [1, 19]. We develop a well-engineered MDLM implementation that significantly improves discrete diffusion log-likelihood; we further improve likelihood using a simple substitution-based parameterization of the reverse diffusion process that enables deriving a Rao-Blackwellized continuous-time variational lower bound (ELBO) with improved tightness. Interestingly, our objective has a simple form: it is a weighted average

For brevity, we drop i from $t(i)$ and $s(i)$ below; in general, s will denote the time step before t .

2.2 Discrete Diffusion Models

Applications of diffusion modeling to discrete data can be broken into two broad categories. First are works that embed discrete structures in continuous space and then perform the Gaussian diffusion defined above on these continuous representations [6, 11, 17, 18, 22, 26, 42]. More related to our method are works that define a diffusion process directly on discrete structures. D3PM [1] introduces a framework with a Markov forward process $q(\mathbf{z}_t|\mathbf{z}_{t-1}) = \text{Cat}(\mathbf{z}_t; Q_t \mathbf{z}_{t-1})$ defined by the multiplication of matrices Q_t over T discrete time steps. This process induces marginals

$$q(\mathbf{z}_t|\mathbf{x}) = \text{Cat}(\mathbf{z}_t; \bar{Q}_t \mathbf{x}) = \text{Cat}(\mathbf{z}_t; Q_t \cdot Q_{t-1} \cdots Q_1 \mathbf{x}) \quad (3)$$

that represent the discrete-state form of (1). Extending this formalism to continuous time (as in (1)) relies on continuous time Markov chain (CTMC) theory [4]. The CTMC framework in turns leads to generalizations of the score matching perspective on diffusion modeling [40] to discrete data [25, 44]. Notably, SEDD [25] connects score-based approaches with ELBO maximization, enabling performant likelihood-based training of score-based models.

3 Simple Masked Diffusion Models

While previous work on discrete diffusion supports general forward processes (e.g., general Q_t in D3PM), absorbing state (i.e., masking) diffusion consistently achieves the best performance [1, 25]. In this work, instead of supporting general noise processes, we focus on masking and derive tight Rao-Blackwellized objectives that outperform general approaches and do not require CTMC theory. In this section, we first define the diffusion process for a categorical random variable. Later in Sec. 3.5, we extend this process to sequences containing multiple such categorical variables. We denote our overall approach as Masked Diffusion Language Models (MDLM).

Notation. We denote scalar discrete random variables with K categories as ‘one-hot’ column vectors and define $\mathcal{V} \in \{\mathbf{x} \in \{0, 1\}^K : \sum_{i=1}^K x_i = 1\}$ as the set of all such vectors. Define $\text{Cat}(\cdot; \boldsymbol{\pi})$ as the categorical distribution over K classes with probabilities given by $\boldsymbol{\pi} \in \Delta^K$, where Δ^K denotes the K -simplex. We also assume that the K -th category corresponds to a special [MASK] token and let $\mathbf{m} \in \mathcal{V}$ be the one-hot vector for this mask, i.e., $\mathbf{m}_K = 1$. Additionally, let $\mathbf{1} = \{1\}^K$ and $\langle \mathbf{a}, \mathbf{b} \rangle$ and $\mathbf{a} \odot \mathbf{b}$ respectively denote the dot and Hadamard products between two vectors \mathbf{a} and \mathbf{b} .

3.1 Interpolating Discrete Diffusion

We restrict our attention to forward processes q that interpolate between clean data $\mathbf{x} \in \mathcal{V}$ and a target distribution $\text{Cat}(\cdot; \boldsymbol{\pi})$, forming a direct extension of Gaussian diffusion in (1). The q define a sequence of increasingly noisy latent variables $\mathbf{z}_t \in \mathcal{V}$, where the time step t runs from $t=0$ (least noisy) to $t=1$ (most noisy). The marginal of \mathbf{z}_t conditioned on \mathbf{x} at time t is

$$q(\mathbf{z}_t|\mathbf{x}) = \text{Cat}(\mathbf{z}_t; \alpha_t \mathbf{x} + (1 - \alpha_t) \boldsymbol{\pi}), \quad (4)$$

where $\alpha_t \in [0, 1]$ is a strictly decreasing function in t , with $\alpha_0 \approx 1$ and $\alpha_1 \approx 0$; see Suppl. D.1 for details. This implies transition probabilities $q(\mathbf{z}_t|\mathbf{z}_s) = \text{Cat}(\mathbf{z}_t; \alpha_{t|s} \mathbf{z}_s + (1 - \alpha_{t|s}) \boldsymbol{\pi})$, where $\alpha_{t|s} = \alpha_t / \alpha_s$. This indicates that during each diffusion step from $s \rightarrow t$, a fraction $(1 - \alpha_{t|s})$ of the probability mass is transferred to the prior distribution $\boldsymbol{\pi}$. The reverse posterior is given as (see Suppl. I.5 for details):

$$q(\mathbf{z}_s|\mathbf{z}_t, \mathbf{x}) = \text{Cat} \left(\mathbf{z}_s; \frac{[\alpha_{t|s} \mathbf{z}_t + (1 - \alpha_{t|s}) \mathbf{1} \boldsymbol{\pi}^\top \mathbf{z}_t] \odot [\alpha_s \mathbf{x} + (1 - \alpha_s) \boldsymbol{\pi}]}{\alpha_t \mathbf{z}_t^\top \mathbf{x} + (1 - \alpha_t) \mathbf{z}_t^\top \boldsymbol{\pi}} \right). \quad (5)$$

While (4) and (5) represent a special case of the more general diffusion processes proposed in D3PM [1], we show below that they yield a simplified variational lower bound objective and admit straightforward continuous time extensions.

3.2 Masked Diffusion

Next, we focus on masking processes and derive a simple Rao-Blackwellized objective for this choice of q . This objective incurs lower variance during training and improves tightness.

3.2.1 Forward Masking Process

In masked (i.e., absorbing state) diffusion, we set $\boldsymbol{\pi} = \mathbf{m}$. At each noising step, t , the input \mathbf{x} transitions to a ‘masked’ state \mathbf{m} with some probability. If an input transitions to \mathbf{m} at any time t' , it will remain in this state for all $t > t'$: $q(\mathbf{z}_t | \mathbf{z}_{t'} = \mathbf{m}) = \text{Cat}(\mathbf{z}_t; \mathbf{m})$. At time T , all inputs are masked with probability 1.

The marginal of the forward process (4) is given by $q(\mathbf{z}_t | \mathbf{x}) = \alpha_t \mathbf{x} + (1 - \alpha_t) \mathbf{m}$. Using properties of the masking process, the posterior $q(\mathbf{z}_s | \mathbf{z}_t, \mathbf{x})$ simplifies (5); see Suppl. A.2:

$$q(\mathbf{z}_s | \mathbf{z}_t, \mathbf{x}) = \begin{cases} \text{Cat}(\mathbf{z}_s; \mathbf{z}_t) & \mathbf{z}_t \neq \mathbf{m}, \\ \text{Cat}\left(\mathbf{z}_s; \frac{(1 - \alpha_s) \mathbf{m} + (\alpha_s - \alpha_t) \mathbf{x}}{1 - \alpha_t}\right) & \mathbf{z}_t = \mathbf{m}. \end{cases} \quad (6)$$

3.2.2 Reverse Unmasking Process

The reverse process inverts the noise process defined by q . We consider both a finite number of steps T , as well as a continuous time model corresponding to $T \rightarrow \infty$. We begin with the discrete-time case for which the generative model is expressed as $p_\theta(\mathbf{x}) = \int_{\mathbf{z}} p_\theta(\mathbf{z}_1) p_\theta(\mathbf{x} | \mathbf{z}_0) \prod_{i=1}^T p_\theta(\mathbf{z}_s | \mathbf{z}_t) d\mathbf{z}_{0:T}$.

The optimal form for $p_\theta(\mathbf{z}_s | \mathbf{z}_t)$ matches the true posterior in (6): this follows immediately from the definition of the diffusion objective in (2), which is a sum of terms of the form $D_{\text{KL}}(q(\mathbf{z}_s | \mathbf{z}_t, \mathbf{x}) || p_\theta(\mathbf{z}_s | \mathbf{z}_t))$. However, (6) is conditioned on \mathbf{x} , which we do not know. Therefore, we introduce a model $\mathbf{x}_\theta(\mathbf{z}_t, t) : \mathcal{V} \times [0, 1] \rightarrow \Delta^K$ that approximates \mathbf{x} with a neural network. We can also omit explicit dependence of \mathbf{x}_θ on time t , which simplifies sampling, yielding a 2x inference speed-up (see Suppl. D.2).

3.2.3 SUBS Parameterization

The specific parameterization for $p_\theta(\mathbf{z}_s | \mathbf{z}_t)$ that we use is

$$p_\theta(\mathbf{z}_s | \mathbf{z}_t) = q(\mathbf{z}_s | \mathbf{z}_t, \mathbf{x} = \mathbf{x}_\theta(\mathbf{z}_t, t)) = \begin{cases} \text{Cat}(\mathbf{z}_s; \mathbf{z}_t), & \mathbf{z}_t \neq \mathbf{m}, \\ \text{Cat}\left(\mathbf{z}_s; \frac{(1 - \alpha_s) \mathbf{m} + (\alpha_s - \alpha_t) \mathbf{x}_\theta(\mathbf{z}_t, t)}{1 - \alpha_t}\right). & \mathbf{z}_t = \mathbf{m}, \end{cases} \quad (7)$$

Furthermore, we induce 2 key properties of the absorbing state diffusion process into our denoising model, $\mathbf{x}_\theta(\mathbf{z}_t, t)$: an input token remains unchanged during reverse diffusion, and the clean input is never masked. We implement these as substitutions to the output of $\mathbf{x}_\theta(\mathbf{z}_t, t)$, hence we call our parameterization SUBS.

Zero Masking Probabilities First, notice that by definition, $\langle \mathbf{x}, \mathbf{m} \rangle = 0$. For this reason, we design the denoising network such that $\langle \mathbf{x}_\theta(\mathbf{z}_t, t), \mathbf{m} \rangle = 0$, i.e., we substitute the logit index corresponding to the [MASK] token with $-\infty$.

Carry-Over Unmasking Second, if \mathbf{z}_t is unmasked, then we desire $\mathbf{x}_\theta(\mathbf{z}_t, t) = \mathbf{z}_t$, i.e., unmasked latents are ‘carried over’. We accomplish this by substituting the output of our network to simply copy unmasked inputs.

In Suppl. B.1, we show that “Zero Masking Probabilities” property simplifies the D3PM’s NELBO (38) to (40), and “Carry-Over Unmasking” further simplifies (40) to (42) whose continuous time equivalent is the simplified NELBO (10). Table 8 shows that each simplification leads to an improved likelihood.

3.3 Rao-Blackwellized Likelihood Bounds

Recall from (2) that the diffusion training objective has the form $\mathcal{L}_{\text{recons}} + \mathcal{L}_{\text{diffusion}} + \mathcal{L}_{\text{prior}}$. For the simplified reverse process in (7), the discrete-time diffusion loss for finite T simplifies to (Suppl. B.1.3):

$$\mathcal{L}_{\text{diffusion}} = \sum_{i=1}^T \mathbb{E}_q [D_{\text{KL}}(q(\mathbf{z}_{s(i)} | \mathbf{z}_{t(i)}, \mathbf{x}) || p_\theta(\mathbf{z}_{s(i)} | \mathbf{z}_{t(i)}))] = \sum_{i=1}^T \mathbb{E}_q \left[\frac{\alpha_{t(i)} - \alpha_{s(i)}}{1 - \alpha_{t(i)}} \log \langle \mathbf{x}_\theta(\mathbf{z}_{t(i)}, \mathbf{x}) \rangle \right]. \quad (8)$$

Note that this objective is simpler and more well-behaved than the expression one would obtain for $D_{\text{KL}}(q(\mathbf{z}_s | \mathbf{z}_t, \mathbf{x}) || p_\theta(\mathbf{z}_s | \mathbf{z}_t))$ under the parameterization induced by using $p_\theta(\mathbf{z}_s | \mathbf{z}_t) = q(\mathbf{z}_s | \mathbf{z}_t, \mathbf{x} = \mathbf{x}_\theta(\mathbf{z}_t, t))$ from (5), which is similar to what is used by D3PM [1] (see Suppl. A.2.4):

$$\left[\frac{\alpha_s - \alpha_t}{1 - \alpha_t} \log \frac{\alpha_t \langle \mathbf{x}_\theta(\mathbf{z}_t, t), \mathbf{m} \rangle + (1 - \alpha_t)}{(1 - \alpha_t) \langle \mathbf{x}_\theta(\mathbf{z}_t, t), \mathbf{x} \rangle} + \frac{1 - \alpha_s}{1 - \alpha_t} \log \frac{(1 - \alpha_s) (\alpha_t \langle \mathbf{x}_\theta(\mathbf{z}_t, t), \mathbf{m} \rangle + (1 - \alpha_t))}{(1 - \alpha_t) (\alpha_s \langle \mathbf{x}_\theta(\mathbf{z}_t, t), \mathbf{m} \rangle + (1 - \alpha_s))} \right] \langle \mathbf{z}_t, \mathbf{m} \rangle. \quad (9)$$

We refer to the process of obtaining (8) in lieu of (9) as a form of Rao-Blackwellization. Specifically, we analytically compute expectations such as $\langle \mathbf{x}_\theta(\mathbf{z}_t, t), \mathbf{m} \rangle = 0$ in order to simplify objective (9) to obtain (8). Without analytical simplifications, a model must learn θ such that $\langle \mathbf{x}_\theta(\mathbf{z}_t, t), \mathbf{m} \rangle = 0$ holds. Unlike in regular Rao-Blackwellization, simplifications are possible because of modeling choices for $\mathbf{x}_\theta(\mathbf{z}_t, t)$ (zero masking probabilities and carry-over unmasking). In that sense, our approach has similarities to graphical modeling, where incorporating conditional independencies into p_θ sets certain log-likelihood terms to zero. However, our approach also empirically helps reduce variance, hence we refer to it as Rao-Blackwellization, somewhat abusing the usual terminology.

3.4 Continuous-Time Likelihood Bounds

Previous works have shown empirically and mathematically that increasing the number of steps T yields a tighter approximation to the ELBO [21]. Following a similar argument, we form an continuous extension of (8) by taking $T \rightarrow \infty$ (see Suppl. B.2), which yields the following NELBO, $\mathcal{L}_{\text{NELBO}}^\infty$:

$$\mathcal{L}_{\text{NELBO}}^\infty = \mathbb{E}_q \int_{t=0}^{t=1} \frac{\alpha'_t}{1-\alpha_t} \log \langle \mathbf{x}_\theta(\mathbf{z}_t, t), \mathbf{x} \rangle dt \quad (10)$$

Invariance to the noise schedule The function α_t is invertible due to the monotonicity assumption in Sec. 3.1, and so we can perform the following change of variables in (10): $\gamma \equiv \log(1 - \alpha_t)$. Thus, the diffusion loss can be equivalently expressed as $\mathcal{L}_{\text{NELBO}}^\infty = -\mathbb{E}_q \int_{\gamma=-\infty}^{\gamma=0} \log \langle \mathbf{x}_\theta(\mathbf{z}_\gamma, \gamma), \mathbf{x} \rangle d\gamma$; see Suppl. D.1.1 for details. This new formulation demonstrates that the diffusion loss is invariant to the functional form of α_t , which we verify empirically in Suppl. D.1.

3.5 Masked Diffusion Language Models

Next, we apply masked diffusion to language modeling over sequences $\mathbf{x}^{1:L}$ of L tokens, with \mathbf{x}^ℓ denoting the ℓ -th token. We make the assumption that the forward noising process is applied independently across a sequence and that, conditioned on a sequence of latents $\mathbf{z}_t^{1:L}$, the denoising process factorizes independently across tokens, i.e., $p_\theta(\mathbf{z}_s^{1:L} | \mathbf{z}_t^{1:L}) = \prod_{\ell=1}^L p_\theta(\mathbf{z}_s^\ell | \mathbf{z}_t^{1:L})$. Thus, we use a single model to compute $\mathbf{x}_\theta^\ell(\mathbf{z}_t^{1:L}, t)$ for each ℓ from a masked sequence \mathbf{z}_t , optimizing:

$$\mathcal{L}_{\text{NELBO}}^\infty = \mathbb{E}_q \int_{t=0}^{t=1} \frac{\alpha'_t}{1-\alpha_t} \sum_{\ell} \log \langle \mathbf{x}_\theta^\ell(\mathbf{z}_t), \mathbf{x}^\ell \rangle dt \quad (11)$$

Interestingly, our objective has a simple form: it is the weighted average of masked language modeling (MLM) losses [10]. Thus our work establishes a connection between generative diffusion models and encoder-only BERT models. Our objective enables principled selection of a (randomized) masking rate, and also endows BERT-style models with principled generation capabilities, see Sec. 6.

3.5.1 Training Considerations for Masked Diffusion

One of the key contributions of our work is a well-engineered implementation of masked diffusion models. Our experiments demonstrate that these improvements greatly boost performance even for methods previously thought to perform poorly, e.g., Austin et al. [1]. Below we briefly summarize these implementation details. First, we find that tokenization is critical to performance. Small vocabularies, such as the 8k vocabulary in Austin et al. [1], result in longer-range dependencies that decrease the performance of both diffusion and AR models. Additionally, by focusing on masked diffusion, we are able to provide a numerically stable implementation of the objective function. Namely, since previous formulations of discrete diffusion were constructed to accommodate a wide range of limiting distributions [1], the objective was implemented by materializing the full transition matrices \bar{Q}_t and posterior probabilities. In contrast, we evaluate $D_{\text{KL}}[q(\mathbf{z}_s | \mathbf{z}_t, \mathbf{x}) || p_\theta(\mathbf{z}_s | \mathbf{z}_t)]$ by examining only the masked token indices rather than comparing the full true and approximate posterior distributions.

Furthermore, we modernize the architecture for the denoising network relative to D3PM [1]. In lieu of the T5 architecture used in D3PM, we use the diffusion transformer (DiT) introduced in Peebles & Xie [32], which integrates time step conditioning into a standard encoder-only transformer [47] and uses rotary positional embeddings [43]. In addition, we implement a low-discrepancy sampler that reduces the variance of the ELBO, similar to Kingma et al. [21] and draws correlated samples t_i rather than performing i.i.d. sampling.

4 Inference and Sampling in Masked Diffusion Language Models

4.1 Efficient Ancestral Sampling

To generate a sequence of length L , the reverse diffusion process starts with the sequence $\mathbf{z}_{t=1}^{1:L}$ where $\mathbf{z}_{t=1}^\ell = \mathbf{m}$, for all $\ell \in \{1, \dots, L\}$. Then the subsequent latents, $\mathbf{z}_t^{1:L}$ are generated by discretizing the reverse diffusion process with some finite T . Given $\mathbf{z}_t^{1:L}$, we construct $\mathbf{z}_s^{1:L}$ by sampling each token \mathbf{z}_s^ℓ independently from the distribution $p_\theta(\mathbf{z}_s^\ell | \mathbf{z}_t^{1:L})$ given in (7).

Note that in the reverse process, unmasked tokens remain unchanged. Thus, if no new tokens in $\mathbf{z}_s^{1:L}$ become unmasked (which can occur often in early denoising stages for large T), then $\mathbf{z}_s^{1:L} = \mathbf{z}_t^{1:L}$. Additionally if the denoising model, $\mathbf{x}_\theta(\mathbf{z}_t^{1:L})$ is not conditioned on time, then we can simply draw a new sample from $p_\theta(\mathbf{z}_{s-1/T}^{1:L} | \mathbf{z}_s^{1:L})$ using the previously computed and cached value $\mathbf{x}_\theta(\mathbf{z}_t^{1:L})$. This means we have effectively ‘skipped’ over the time step s , saving a function call to the denoising network. Note that SEDD [25] does not support this caching because the denoising network models time-dependent rates, which requires conditioning on time.

4.2 Semi-Autoregressive Masked Diffusion Language Models

Our method also admits an effective semi-autoregressive (SAR) decoding method that allows the model to generate sequences of arbitrary length. Let $\tilde{\mathbf{x}}^{1:L}$ represent the output from sampling a sequence of L tokens using the reverse diffusion process described above. To generate additional $L' < L$ tokens, we propose a generation algorithm in which the latter $L - L'$ tokens $\tilde{\mathbf{x}}^{L':L-L'}$ are used as a prefix for an additional round of generation. Given the carry-over unmasking described in Sec. 3.2.3, these prefix tokens will simply be copied over at each decoding step. The remaining tokens are generated as above with $\mathbf{z}_s^\ell \sim p_\theta(\mathbf{z}_s^\ell | \mathbf{z}_t^{L':L+L'})$ for all $\ell \in \{L+1, \dots, L+L'\}$, with $\mathbf{z}_1^{L':L-L'}$ initialized to $\tilde{\mathbf{x}}^{L':L-L'}$ as opposed to being initialized as masked tokens \mathbf{m} . At the end of this process, we have produced $L+L'$ tokens $\text{concat}[\tilde{\mathbf{x}}^{1:L}, \tilde{\mathbf{x}}^{L+1:L+L'}]$, where $\text{concat}[\cdot]$ denotes concatenation along the sequence length dimension. This process can repeat indefinitely, with the prefix shifted for every new round of generation.

5 Experiments

5.1 Masked Diffusion Language Models

Experimental Setup We evaluate MDLM as a generative model of language and as a representation model via fine-tuning on downstream tasks.

For language modeling likelihood evaluation, we conduct experiments on two datasets: The One Billion Words Dataset (LM1B; [5]) and OpenWebText (OWT; [13]). We use the `bert-base-uncased` tokenizer for One Billion Words, and report perplexities on the test split. Models have a context size of 128. For OWT, which does not have a pre-defined split, we reserve the last 100K documents as a held-out validation set and report perplexities on this set. We use the GPT2 tokenizer [35] for OWT. Models have a context size of 1,024. We utilize the transformer architecture from Lou et al. [25], which augments the diffusion transformer [32] with rotary embeddings [43]. MDLM was trained for 1M or 10M steps (corresponding to 33B, 327B tokens, respectively) on LM1B and 1M steps on OWT (which corresponds to 262B tokens). The corresponding AR baseline was trained for half the number of steps to ensure similar number of tokens seen (details in Suppl. C.2). Full hyperparameters are given in Suppl. C.4. On OWT, we train with and without time step conditioning.

For representation learning, we pre-train models on the C4 dataset [36], then fine-tune and evaluate models on the GLUE benchmark [50]. Models have a context size of 128. We use the `bert-base-uncased` tokenizer for the representation learning experiments. We utilize the MosaicBERT architecture from Portes et al. [33], an extension of the original BERT architecture [10]. We pre-train a bidirectional MosaicBERT using an MLM objective for 37B tokens of C4, as well as a causal variant on the same data. We further fine-tune MosaicBERT model using the MDLM for 327M tokens, less than 1% of the pre-training data. We provide the full hyperparameters in Suppl. C.6.

Likelihood Evaluation On LM1B, MDLM outperforms all previous diffusion methods (Table 1). Compared to the SEDD baseline reported by Lou et al. [25], trained for 66B tokens, MDLM, which

Table 1: Test perplexities (PPL; \downarrow) on LM1B. \dagger Reported in He et al. [19]. Best diffusion value is bolded.

		Parameters	PPL (\downarrow)
<i>Autoregressive</i>	Transformer-X Base [9]	0.46B	23.5
	OmniNet _T [46]	100M	21.5
<i>Diffusion</i>	BERT-Mouth [49]	110M	≤ 142.89
	D3PM (absorb) [1]	70M	≤ 77.50
	Diffusion-LM [22] \dagger	80M	≤ 118.62
	DiffusionBert [19]	110M	≤ 63.78
	SEDD [25] (33B tokens)	110M	≤ 32.79
<i>Autoregressive (Retrained)</i>	Transformer (33B tokens)	110M	22.32
	Transformer (327B tokens)		20.86
<i>Diffusion (Ours)</i>	MDLM (33B tokens)	110M	≤ 27.04
	MDLM (327B tokens)		$\leq \mathbf{23.00}$

Table 3: Zero-shot validation perplexities (\downarrow) of models trained for 524B tokens on OWT. All perplexities for diffusion models are upper bounds.

	PTB	Wikitext	LM1B	Lambada	AG News	Pubmed	Arxiv
AR (Retrained)	82.05	25.75	51.25	51.28	52.09	49.01	41.73
SEDD (Retrained)	100.09	34.28	68.20	49.86	62.09	44.53	38.48
MDLM (Ours)	95.26	32.83	67.01	47.52	61.15	41.89	37.37

Table 4: GLUE evaluation results. Evaluation measures (\uparrow) are F1 score for QQP and MRPC, Spearman correlations for STS-B, and accuracy for the rest. For MNLI, we report match/mismatch accuracies.

	MNLI (m/mm)	QQP	QNLI	SST-2	COLA	STS-B	MRPC	RTE	Avg
AR	80.94/80.78	86.98	86.16	90.14	33.43	84.32	83.88	47.29	74.88
BERT	84.43/85.35	88.41	90.46	92.20	54.81	88.41	89.16	61.37	81.62
+MDLM-FT	84.76/85.07	88.49	90.30	92.20	57.69	87.48	90.53	62.09	82.06

we train for the same amount, achieves a 17% improvement on the perplexity bound. Finally, MDLM gets within 14% of an AR baseline and continues to improve with more training. We see the same trend for models trained on OWT, a larger dataset, shown in Table 2 – MDLM outperforms prior diffusion methods, closing the gap towards AR models. Results on OWT time step conditioning are in Table 12, Suppl. D.5 where we find that models trained with and without time conditioning attain similar perplexities. Additionally, Figure 3 demonstrates the reduced variance we achieve from our objective, when compared to previous masked diffusion models, such as SEDD [25].

Zero-Shot Likelihood Evaluation We also explore models’ ability to generalize by taking models trained on OWT and evaluating how well they model unseen datasets. We compare the perplexities of our MDLM with a SEDD parameterization and an AR Transformer language model. Our zero-shot datasets include the validation splits of Penn Tree Bank (PTB; [28]), Wikitext [29], LM1B, Lambada [31], AG News [51], and Scientific Papers (Pubmed and Arxiv subsets; [7]). Full experimental details are available in Suppl. C.4.

MDLM consistently outperforms the SEDD diffusion parameterization. In some cases, e.g., for Lambada and Scientific Papers, MDLM attains better perplexity than AR. We hypothesize that these datasets are farther from OWT, and that diffusion models may be more robust to out-of-domain evaluation due to the unmasking-based objective.

Table 2: Test perplexities (PPL; \downarrow) on OWT for models trained for 262B tokens. \dagger denotes retrained models.

	PPL (\downarrow)
AR \dagger	17.54
SEDD \dagger	≤ 24.10
MDLM (Ours)	$\leq \mathbf{23.21}$

Table 6: Test perplexities (PPL; \downarrow) of generative fine-tuning of the Caduceus MLM [38] on the HG38 reference genome. Best diffusion model values are bolded. Error bars indicate the difference between the maximum and minimum values across 5 random seeds used for fine-tuning.

		Params	PPL (\downarrow)
<i>Autoregressive (Retrained)</i>	Mamba	465K	$3.067 \pm .0104$
	HyenaDNA	433K	$3.153 \pm .001$
<i>Diffusion (Retrained)</i>	Plaid	507K	$\leq 3.240 \pm .005$
	SEDD	467K	$\leq 3.216 \pm .003$
<i>Diffusion (Ours)</i>	MDLM	467K	$\leq \mathbf{3.199} \pm .010$

Downstream Task Evaluation We find that BERT fine-tuned with MDLM to be a generative model results in strong perplexities while preserving performance on downstream tasks. On the C4 validation set, the AR model attains perplexity (PPL) of 22, the pre-trained BERT attains a PPL upper bound of 78 (evaluated using the MDLM variational bound), and BERT + MDLM-FT attains a PPL upper bound of 35. In Table 4, we further find that BERT + MDLM fine-tuning has no degradation in downstream GLUE performance compared to the BERT initialization. While the perplexity of our method is higher than the AR baseline, the downstream task performance is significantly better.

Semi-Autoregressive Modeling To test the SAR decoding algorithm presented in Sec. 4.2, we compare to SSD-LM [18] a diffusion model that was designed to generate blocks of text autoregressively. We generate 200 sequences of length 2048 tokens on a single 3090 GPU and evaluate generative perplexity under a pre-trained GPT-2 [35] model. The SSD-LM sequences are generated using blocks of 25 tokens (as implemented in their pre-trained model) and the MDLM sequences are generated using $L' = 512$. In Table 5, we find that in addition to achieving better generative perplexity, MDLM enables ~ 25 - 30 x faster SAR decoding relative to SSD-LM.

5.2 Masked Diffusion DNA Models

We also explore the use of our generative formulation in conjunction with Structured State Space models [16]. Namely, we build on the recently proposed Caduceus [38] model, which uses as a backbone the data-dependent SSM Mamba block [15].

Table 5: Semi-AR generative perplexity (Gen. PPL; \downarrow) for sequences of 2048 tokens.

	Gen. PPL (\downarrow)	Sec/Seq (\downarrow)
SSD-LM	35.43	2473.9
MDLM (Ours)	27.18	89.3

Experimental Setup We pre-train the encoder-only Caduceus [38], which is an MLM, on the HG38 human reference genome [8] and perform fine-tuning using our diffusion parameterization. We use a context length of 1024 tokens and follow Schiff et al. [38] for the experimental setup, other than learning rate which was reduced to $1e-3$. See Suppl. C.7 for full experimental details. We assess both generative performance using perplexity and downstream performance on Genomics Benchmarks [14] across language diffusion paradigms and AR models.

Generative Performance We fine-tune the Caduceus MLM across diffusion parameterizations and compare perplexities against AR models. We report perplexity values in Table 6. MDLM outperforms all other diffusion language modeling schemes.

Downstream Task Fine-tuning We perform downstream evaluation with the Genomics Benchmarks [14], a recently proposed benchmark with eight regulatory element classification tasks. As shown in Table 7, our generative fine-tuning paradigm preserves or improves upon downstream performance from MLM pre-training. Absorbing-state diffusion methods outperform Plaid across tasks except for the simplest task Human vs. Worm, where all methods have roughly the same performance. For tasks where the input is a biased subsample of the full genome, we observe that the correlation between perplexity and downstream performance is weaker; see Suppl. C.7.

Table 7: Genomic Benchmarks. Top-1 accuracy (\uparrow) across 5-fold cross-validation (CV) for a pre-trained AR Mamba, and a pre-trained Caduceus model fine-tuned with different diffusion parameterizations. The best values per task are bolded and the second best are italicized. Error bars indicate the difference between the maximum and minimum values across 5 random seeds used for CV.

Model Fine-Tuning Objective (Parameter Count)	Mamba AR (465K)	Caduceus MLM (467K)	Caduceus Plaid (507k)	Caduceus SEDD (467k)	Caduceus MDLM (ours) (467k)
Mouse Enhancers	0.763 (± 0.008)	0.810 (± 0.016)	0.745 (± 0.079)	0.784 (± 0.058)	<i>0.795</i> (± 0.029)
Coding vs. Intergenic	0.897 (± 0.004)	0.913 (± 0.003)	<i>0.908</i> (± 0.003)	0.913 (± 0.005)	0.913 (± 0.003)
Human vs. Worm	0.967 (± 0.002)	<i>0.970</i> (± 0.002)	0.971 (± 0.001)	<i>0.970</i> (± 0.003)	<i>0.970</i> (± 0.003)
Human Enhancers Cohn	0.734 (± 0.027)	<i>0.737</i> (± 0.001)	<i>0.743</i> (± 0.010)	0.746 (± 0.015)	<i>0.743</i> (± 0.016)
Human Enhancer Ensembl	0.856 (± 0.003)	0.907 (± 0.000)	0.885 (± 0.003)	<i>0.905</i> (± 0.006)	0.899 (± 0.004)
Human Regulatory	0.861 (± 0.008)	0.874 (± 0.003)	<i>0.868</i> (± 0.010)	0.828 (± 0.037)	<i>0.868</i> (± 0.004)
Human OCR Ensembl	0.806 (± 0.005)	<i>0.821</i> (± 0.000)	0.820 (± 0.004)	0.816 (± 0.008)	0.823 (± 0.008)
Human NonTATA Promoters	0.926 (± 0.008)	<i>0.935</i> (± 0.014)	<i>0.935</i> (± 0.007)	<i>0.935</i> (± 0.014)	0.940 (± 0.007)

5.3 Ablation Analysis

In Table 8, we can see the effect of our streamlined masked diffusion implementation. The improvements described in Sec. 3.5.1 allow us to greatly reduce perplexity of previously discounted models, such as D3PM (see the bottom row of this table, which is mathematically equivalent to the D3PM formulation). While most works assumed that D3PM achieves mediocre log-likelihoods, we show that is incorrect: our re-implementation almost matches state-of-the-art score-based methods. This introduces a new strong baseline that opens new research opportunities. Additionally, in Table 8, we ablate different components of MDLM. We observe that the perplexity for MDLM trained with a discrete $T = 1000$ marginally worsens by 0.1 compared to MDLM trained in continuous time. Additionally, removing the “carry over” operation from the SUBS parameterization increases the perplexity by 1.5 points. However, further removing the “zero masking” operation does not lead to any meaningful change in perplexity.

We provide further ablations for the continuous time formulation in the Appendix, showing in Table 11 that for a pre-trained model, at inference, increasing T yields better likelihoods.

6 Discussion, Prior Work, and Conclusion

Comparison to D3PM Masked diffusion is a strict subset of D3PM [1]; setting $Q_{t|s} = \alpha_{t|s}I + (1 - \alpha_{t|s})\mathbf{1m}^\top$ in their framework yields our forward diffusion. We improve over D3PM in three ways: (1) we adopt the SUBS parameterization for $p_\theta(\mathbf{z}_s|\mathbf{z}_t)$; (2) this allows us to derive a simplified objective that analytically simplifies certain expectations to zero; (3) we adopt well-engineered training recipes that improve performance. Both (1) and (2) are possible because we focus on masking instead of developing a general discrete diffusion framework. Surprisingly, (3) has the largest contribution to performance.

Table 8: Test perplexities (PPL; \downarrow) for MDLM ablations on LM1B. For the discrete-time models, we use $T = 1000$. Standard deviation is measured over 5 seeds during evaluation.

	PPL (\leq)
MDLM (46)	27.04 \pm .01
w/o Continuous time (42)	27.19 \pm .07
& w/o carry-over (40)	28.56 \pm .15
& w/o zero masking (38)	28.51 \pm .15

Comparison to CTMC Most implementations of diffusion work best in continuous time. However, extending D3PM in this way requires computing the limit of the product of an infinite number of matrices $Q_T \cdot Q_{T-1} \cdots Q_t$ as $T \rightarrow \infty$, which requires advanced CTMC theory [4]. Our work describes simple continuous-time formulations for the most common noise processes (e.g., masking and uniform π), thus helping make an important part of the literature more accessible. Our results remain compatible with CTMC: we effectively use rate matrices $R_t = \alpha'_t(\mathbf{1m}^\top - I)$.

Comparison to Score Estimation Score-based approaches to diffusion [40] extend to discrete states, although they typically further build upon advanced CTMC theory. In particular, SEDD [25] derives and optimizes an ELBO that is a function of the score model, obtaining state-of-the-art log-likelihoods among diffusion models. We use a much simpler approach that requires no advanced theory.

Comparison to BERT Our work provides a principled way of making BERT generative when trained with randomized masking rates. Previous work on generating from BERT used Gibbs sampling or ad-hoc methods [12, 24, 49]. The connection between BERT and diffusion was first made by Austin et al. [1]: their objective effectively involves unmasking. He et al. [19] additionally starts training from a pretrained BERT. However, both works use an objective that is similar to (9), which is less numerically stable than our objective (see Section 3.5.1). Austin et al. [1] describe in their appendix how their ELBO can simplify to a weighted masking (MLM) loss similar to (8), but using a more complex formula for the weights. However, they do not train with that objective. Our work derives a simpler expression for the average of MLM losses, implements it, and obtains better likelihoods.

Conclusion In this work, we explore masked diffusion. With a well-engineered implementation that supports a simple variational objective, we attain state-of-the-art diffusion perplexities on language benchmarks and demonstrate how to efficiently convert BERT-style encoders into generative models. Given we are working on language modeling, we carry any of the inherent risks and opportunities that come with this line of research.

References

- [1] Jacob Austin, Daniel D Johnson, Jonathan Ho, Daniel Tarlow, and Rianne Van Den Berg. Structured denoising diffusion models in discrete state-spaces. *Advances in Neural Information Processing Systems*, 34:17981–17993, 2021.
- [2] Pavel Avdeyev, Chenlai Shi, Yuhao Tan, Kseniia Dudnyk, and Jian Zhou. Dirichlet diffusion score model for biological sequence generation. In *International Conference on Machine Learning*, pp. 1276–1301. PMLR, 2023.
- [3] Žiga Avsec, Vikram Agarwal, Daniel Visentin, Joseph R Ledsam, Agnieszka Grabska-Barwinska, Kyle R Taylor, Yannis Assael, John Jumper, Pushmeet Kohli, and David R Kelley. Effective gene expression prediction from sequence by integrating long-range interactions. *Nature methods*, 18(10):1196–1203, 2021.
- [4] Andrew Campbell, Joe Benton, Valentin De Bortoli, Thomas Rainforth, George Deligiannidis, and Arnaud Doucet. A continuous time framework for discrete denoising models. *Advances in Neural Information Processing Systems*, 35:28266–28279, 2022.
- [5] Ciprian Chelba, Tomas Mikolov, Mike Schuster, Qi Ge, Thorsten Brants, Phillipp Koehn, and Tony Robinson. One billion word benchmark for measuring progress in statistical language modeling, 2014.
- [6] Ting Chen, Ruixiang Zhang, and Geoffrey Hinton. Analog bits: Generating discrete data using diffusion models with self-conditioning. *arXiv preprint arXiv:2208.04202*, 2022.
- [7] Arman Cohan, Franck Dernoncourt, Doo Soon Kim, Trung Bui, Seokhwan Kim, Walter Chang, and Nazli Goharian. A discourse-aware attention model for abstractive summarization of long documents. *Proceedings of the 2018 Conference of the North American Chapter of the Association for Computational Linguistics: Human Language Technologies, Volume 2 (Short Papers)*, 2018. doi: 10.18653/v1/n18-2097. URL <http://dx.doi.org/10.18653/v1/n18-2097>.
- [8] Genome Reference Consortium. Genome reference consortium human build 37 (grch37). *Database (GenBank or RefSeq)*, 2009.
- [9] Zihang Dai, Zhilin Yang, Yiming Yang, Jaime Carbonell, Quoc V Le, and Ruslan Salakhutdinov. Transformer-xl: Attentive language models beyond a fixed-length context. *arXiv preprint arXiv:1901.02860*, 2019.
- [10] Jacob Devlin, Ming-Wei Chang, Kenton Lee, and Kristina Toutanova. Bert: Pre-training of deep bidirectional transformers for language understanding. *arXiv preprint arXiv:1810.04805*, 2018.
- [11] Sander Dieleman, Laurent Sartran, Arman Roshannai, Nikolay Savinov, Yaroslav Ganin, Pierre H Richemond, Arnaud Doucet, Robin Strudel, Chris Dyer, Conor Durkan, et al. Continuous diffusion for categorical data. *arXiv preprint arXiv:2211.15089*, 2022.

- [12] Marjan Ghazvininejad, Omer Levy, Yinhan Liu, and Luke Zettlemoyer. Mask-predict: Parallel decoding of conditional masked language models. In Kentaro Inui, Jing Jiang, Vincent Ng, and Xiaojun Wan (eds.), *Proceedings of the 2019 Conference on Empirical Methods in Natural Language Processing and the 9th International Joint Conference on Natural Language Processing (EMNLP-IJCNLP)*, pp. 6112–6121, Hong Kong, China, November 2019. Association for Computational Linguistics. doi: 10.18653/v1/D19-1633. URL <https://aclanthology.org/D19-1633>.
- [13] Aaron Gokaslan, Vanya Cohen, Ellie Pavlick, and Stefanie Tellex. Openwebtext corpus. <http://Skyllion007.github.io/OpenWebTextCorpus>, 2019.
- [14] Katarína Grešová, Vlastimil Martinek, David Čechák, Petr Šimeček, and Panagiotis Alexiou. Genomic benchmarks: a collection of datasets for genomic sequence classification. *BMC Genomic Data*, 24(1):25, 2023.
- [15] Albert Gu and Tri Dao. Mamba: Linear-time sequence modeling with selective state spaces. *arXiv preprint arXiv:2312.00752*, 2023.
- [16] Albert Gu, Karan Goel, and Christopher Ré. Efficiently modeling long sequences with structured state spaces. *arXiv preprint arXiv:2111.00396*, 2021.
- [17] Ishaan Gulrajani and Tatsunori B Hashimoto. Likelihood-based diffusion language models. *Advances in Neural Information Processing Systems*, 36, 2024.
- [18] Xiaochuang Han, Sachin Kumar, and Yulia Tsvetkov. Ssd-lm: Semi-autoregressive simplex-based diffusion language model for text generation and modular control. *arXiv preprint arXiv:2210.17432*, 2022.
- [19] Zhengfu He, Tianxiang Sun, Kuanning Wang, Xuanjing Huang, and Xipeng Qiu. Diffusionbert: Improving generative masked language models with diffusion models. *arXiv preprint arXiv:2211.15029*, 2022.
- [20] Jonathan Ho, Ajay Jain, and Pieter Abbeel. Denoising diffusion probabilistic models. *Advances in neural information processing systems*, 33:6840–6851, 2020.
- [21] Diederik Kingma, Tim Salimans, Ben Poole, and Jonathan Ho. Variational diffusion models. *Advances in neural information processing systems*, 34:21696–21707, 2021.
- [22] Xiang Li, John Thickstun, Ishaan Gulrajani, Percy S Liang, and Tatsunori B Hashimoto. Diffusion-lm improves controllable text generation. *Advances in Neural Information Processing Systems*, 35:4328–4343, 2022.
- [23] Xuanlin Li, Brandon Trabucco, Dong Huk Park, Michael Luo, Sheng Shen, Trevor Darrell, and Yang Gao. Discovering non-monotonic autoregressive orderings with variational inference. *arXiv preprint arXiv:2110.15797*, 2021.
- [24] Yi Liao, Xin Jiang, and Qun Liu. Probabilistically masked language model capable of autoregressive generation in arbitrary word order. In Dan Jurafsky, Joyce Chai, Natalie Schluter, and Joel Tetreault (eds.), *Proceedings of the 58th Annual Meeting of the Association for Computational Linguistics*, pp. 263–274, Online, July 2020. Association for Computational Linguistics. doi: 10.18653/v1/2020.acl-main.24. URL <https://aclanthology.org/2020.acl-main.24>.
- [25] Aaron Lou, Chenlin Meng, and Stefano Ermon. Discrete diffusion language modeling by estimating the ratios of the data distribution. *arXiv preprint arXiv:2310.16834*, 2023.
- [26] Justin Lovelace, Varsha Kishore, Chao Wan, Eliot Shekhtman, and Kilian Q Weinberger. Latent diffusion for language generation. *Advances in Neural Information Processing Systems*, 36, 2024.
- [27] Vincent Mallet and Jean-Philippe Vert. Reverse-complement equivariant networks for dna sequences. *Advances in neural information processing systems*, 34:13511–13523, 2021.
- [28] Mitch Marcus, Beatrice Santorini, and Mary Ann Marcinkiewicz. Building a large annotated corpus of english: The penn treebank. *Computational linguistics*, 19(2):313–330, 1993.

- [29] Stephen Merity, Caiming Xiong, James Bradbury, and Richard Socher. Pointer sentinel mixture models, 2016.
- [30] Eric Nguyen, Michael Poli, Marjan Faizi, Armin Thomas, Michael Wornow, Callum Birch-Sykes, Stefano Massaroli, Aman Patel, Clayton Rabideau, Yoshua Bengio, et al. Hyenadna: Long-range genomic sequence modeling at single nucleotide resolution. *Advances in neural information processing systems*, 36, 2024.
- [31] Denis Paperno, Germán Kruszewski, Angeliki Lazaridou, Ngoc Quan Pham, Raffaella Bernardi, Sandro Pezzelle, Marco Baroni, Gemma Boleda, and Raquel Fernandez. The LAMBADA dataset: Word prediction requiring a broad discourse context. In *Proceedings of the 54th Annual Meeting of the Association for Computational Linguistics (Volume 1: Long Papers)*, pp. 1525–1534, Berlin, Germany, August 2016. Association for Computational Linguistics. URL <http://www.aclweb.org/anthology/P16-1144>.
- [32] William Peebles and Saining Xie. Scalable diffusion models with transformers. In *Proceedings of the IEEE/CVF International Conference on Computer Vision*, pp. 4195–4205, 2023.
- [33] Jacob Portes, Alex Trott, Sam Havens, Daniel King, Abhinav Venigalla, Moin Nadeem, Nikhil Sardana, Daya Khudia, and Jonathan Frankle. Mosaicbert: A bidirectional encoder optimized for fast pretraining, 2024.
- [34] Ofir Press, Noah A. Smith, and Mike Lewis. Train short, test long: Attention with linear biases enables input length extrapolation, 2022.
- [35] Alec Radford, Jeff Wu, Rewon Child, David Luan, Dario Amodei, and Ilya Sutskever. Language models are unsupervised multitask learners. 2019.
- [36] Colin Raffel, Noam Shazeer, Adam Roberts, Katherine Lee, Sharan Narang, Michael Matena, Yanqi Zhou, Wei Li, and Peter J. Liu. Exploring the limits of transfer learning with a unified text-to-text transformer. *J. Mach. Learn. Res.*, 21(1), jan 2020. ISSN 1532-4435.
- [37] Subham Sekhar Sahoo, Aaron Gokaslan, Chris De Sa, and Volodymyr Kuleshov. Diffusion models with learned adaptive noise. *arXiv preprint arXiv:2312.13236*, 2023.
- [38] Yair Schiff, Chia-Hsiang Kao, Aaron Gokaslan, Tri Dao, Albert Gu, and Volodymyr Kuleshov. Caduceus: Bi-directional equivariant long-range dna sequence modeling. *arXiv preprint arXiv:2403.03234*, 2024.
- [39] Jascha Sohl-Dickstein, Eric Weiss, Niru Maheswaranathan, and Surya Ganguli. Deep unsupervised learning using nonequilibrium thermodynamics. In *International conference on machine learning*, pp. 2256–2265. PMLR, 2015.
- [40] Yang Song and Stefano Ermon. Generative modeling by estimating gradients of the data distribution. *Advances in neural information processing systems*, 32, 2019.
- [41] Yang Song, Jascha Sohl-Dickstein, Diederik P Kingma, Abhishek Kumar, Stefano Ermon, and Ben Poole. Score-based generative modeling through stochastic differential equations. *arXiv preprint arXiv:2011.13456*, 2020.
- [42] Robin Strudel, Corentin Tallec, Florent Alché, Yilun Du, Yaroslav Ganin, Arthur Mensch, Will Grathwohl, Nikolay Savinov, Sander Dieleman, Laurent Sifre, et al. Self-conditioned embedding diffusion for text generation. *arXiv preprint arXiv:2211.04236*, 2022.
- [43] Jianlin Su, Yu Lu, Shengfeng Pan, Ahmed Murtadha, Bo Wen, and Yunfeng Liu. Roformer: Enhanced transformer with rotary position embedding. *arXiv preprint arXiv:2104.09864*, 2021.
- [44] Haoran Sun, Lijun Yu, Bo Dai, Dale Schuurmans, and Hanjun Dai. Score-based continuous-time discrete diffusion models. *arXiv preprint arXiv:2211.16750*, 2022.
- [45] Zhiqing Sun and Yiming Yang. Difusco: Graph-based diffusion solvers for combinatorial optimization. *Advances in Neural Information Processing Systems*, 36:3706–3731, 2023.

- [46] Yi Tay, Mostafa Dehghani, Vamsi Aribandi, Jai Gupta, Philip M Pham, Zhen Qin, Dara Bahri, Da-Cheng Juan, and Donald Metzler. Omninet: Omnidirectional representations from transformers. In *International Conference on Machine Learning*, pp. 10193–10202. PMLR, 2021.
- [47] Ashish Vaswani, Noam Shazeer, Niki Parmar, Jakob Uszkoreit, Llion Jones, Aidan N Gomez, Łukasz Kaiser, and Illia Polosukhin. Attention is all you need. *Advances in neural information processing systems*, 30, 2017.
- [48] Clement Vignac, Igor Krawczuk, Antoine Siraudin, Bohan Wang, Volkan Cevher, and Pascal Frossard. Digress: Discrete denoising diffusion for graph generation. *arXiv preprint arXiv:2209.14734*, 2022.
- [49] Alex Wang and Kyunghyun Cho. Bert has a mouth, and it must speak: Bert as a markov random field language model. *arXiv preprint arXiv:1902.04094*, 2019.
- [50] Alex Wang, Amanpreet Singh, Julian Michael, Felix Hill, Omer Levy, and Samuel R. Bowman. GLUE: A multi-task benchmark and analysis platform for natural language understanding. In *International Conference on Learning Representations*, 2019. URL <https://openreview.net/forum?id=rJ4km2R5t7>.
- [51] Xiang Zhang, Junbo Jake Zhao, and Yann LeCun. Character-level convolutional networks for text classification. In *NIPS*, 2015.
- [52] Hannah Zhou, Avanti Shrikumar, and Anshul Kundaje. Towards a better understanding of reverse-complement equivariance for deep learning models in genomics. In *Machine Learning in Computational Biology*, pp. 1–33. PMLR, 2022.

Contents

1	Introduction	1
2	Background	2
2.1	Diffusion Models	2
2.2	Discrete Diffusion Models	3
3	Simple Masked Diffusion Models	3
3.1	Interpolating Discrete Diffusion	3
3.2	Masked Diffusion	3
3.3	Rao-Blackwellized Likelihood Bounds	4
3.4	Continuous-Time Likelihood Bounds	5
3.5	Masked Diffusion Language Models	5
4	Inference and Sampling in Masked Diffusion Language Models	6
4.1	Efficient Ancestral Sampling	6
4.2	Semi-Autoregressive Masked Diffusion Language Models	6
5	Experiments	6
5.1	Masked Diffusion Language Models	6
5.2	Masked Diffusion DNA Models	8
5.3	Ablation Analysis	9
6	Discussion, Prior Work, and Conclusion	9
	Appendices	15
	Appendix A Discrete time ELBO	15
A.1	Generic case	15
A.2	Absorbing state	16
	Appendix B MDLM	19
B.1	Rao-Blackwellization	19
B.2	Continuous Time	20
	Appendix C Experimental details	21
C.1	Likelihood Evaluation	21
C.2	Avg. Number of Tokens seen	21
C.3	Low discrepancy sampler	21
C.4	Language Modeling	21
C.5	Zeroshot Likelihood	22
C.6	Representation Learning	22

C.7 Diffusion DNA Models	22
Appendix D Additional Experiments	23
D.1 Noise schedule parameterization	23
D.2 Faster sampling with caching	24
D.3 LM1B ablations	25
D.4 Train NLL curves on OWT	25
D.5 Time-conditioning ablation on OWT	26

Appendices

Appendix A Discrete time ELBO

This section is organized as follows: First, we derive the expressions for the true posterior and the approximate posterior as outlined in Suppl. A.1. We then simplify these expressions specifically for the case of absorbing state diffusion in Suppl. A.2. Finally, we derive the expression for the ELBO for absorbing state diffusion in Suppl. A.2.3.

A.1 Generic case

Given the state transition matrix Q_t , prior $\boldsymbol{\pi}$, and the latent variables \mathbf{z}_s and \mathbf{z}_t , where $s < t$, let

$$Q_{t|s} = \alpha_{t|s} \mathbf{I}_n + (1 - \alpha_{t|s}) \mathbf{1} \boldsymbol{\pi}^\top. \quad (12)$$

A.1.1 $q(\mathbf{z}_t | \mathbf{z}_s)$

Thus, the marginals in (3) correspond to the following forward process:

$$\begin{aligned} q(\mathbf{z}_t | \mathbf{z}_s) &= \text{Cat}(\mathbf{z}_t; Q_{t|s}^\top \mathbf{z}_s) \\ &= \text{Cat}(\mathbf{z}_t; [\alpha_{t|s} \mathbf{I}_n + (1 - \alpha_{t|s}) \mathbf{1} \boldsymbol{\pi}^\top]^\top \mathbf{z}_s) \\ &= \text{Cat}(\mathbf{z}_t; \alpha_{t|s} \mathbf{z}_s + (1 - \alpha_{t|s}) \boldsymbol{\pi} \mathbf{1}^\top \mathbf{z}_s) \quad \because \mathbf{1}^\top \mathbf{z}_s = 1 \\ &= \text{Cat}(\mathbf{z}_t; \alpha_{t|s} \mathbf{z}_s + (1 - \alpha_{t|s}) \boldsymbol{\pi}). \end{aligned} \quad (13)$$

The above equation indicates that during each diffusion step from $s \rightarrow t$, a fraction $(1 - \alpha_{t|s})$ of the probability mass is transferred to the prior distribution $\boldsymbol{\pi}$.

A.1.2 $q(\mathbf{z}_s | \mathbf{z}_t, \mathbf{x})$

Austin et al. [1] show that the posterior corresponding to (13) is given as follows:

$$q(\mathbf{z}_s | \mathbf{z}_t, \mathbf{x}) = \text{Cat} \left(\mathbf{z}_s; \frac{Q_{t|s} \mathbf{z}_t \odot Q_s^\top \mathbf{x}}{\mathbf{z}_t^\top Q_t^\top \mathbf{x}} \right), \quad (14)$$

which we simplify to the following:

$$\begin{aligned} & q(\mathbf{z}_s | \mathbf{z}_t, \mathbf{x}) \\ &= \text{Cat} \left(\mathbf{z}_s; \frac{[\alpha_{t|s} \mathbf{I}_n + (1 - \alpha_{t|s}) \mathbf{1} \boldsymbol{\pi}^\top] \mathbf{z}_t \odot [\alpha_s \mathbf{I}_n + (1 - \alpha_s) \mathbf{1} \boldsymbol{\pi}^\top]^\top \mathbf{x}}{\mathbf{z}_t^\top [\alpha_t \mathbf{I}_n + (1 - \alpha_t) \mathbf{1} \boldsymbol{\pi}^\top]^\top \mathbf{x}} \right) \\ &= \text{Cat} \left(\mathbf{z}_s; \frac{[\alpha_{t|s} \mathbf{z}_t + (1 - \alpha_{t|s}) \mathbf{1} \boldsymbol{\pi}^\top \mathbf{z}_t] \odot [\alpha_s \mathbf{x} + (1 - \alpha_s) \boldsymbol{\pi}]}{\mathbf{z}_t^\top [\alpha_t \mathbf{x} + (1 - \alpha_t) \boldsymbol{\pi} \mathbf{1}^\top \mathbf{x}]} \right) \\ &= \text{Cat} \left(\mathbf{z}_s; \frac{[\alpha_{t|s} \mathbf{z}_t + (1 - \alpha_{t|s}) \mathbf{1} \boldsymbol{\pi}^\top \mathbf{z}_t] \odot [\alpha_s \mathbf{x} + (1 - \alpha_s) \boldsymbol{\pi}]}{\alpha_t \mathbf{z}_t^\top \mathbf{x} + (1 - \alpha_t) \mathbf{z}_t^\top \boldsymbol{\pi}} \right). \quad \because \mathbf{1}^\top \mathbf{x} = 1 \end{aligned} \quad (15)$$

A.1.3 $p_\theta(\mathbf{z}_s|\mathbf{z}_t)$

Austin et al. [1] approximate the reverse process in the following manner:

$$p_\theta(\mathbf{z}_s|\mathbf{z}_t) = q(\mathbf{z}_s|\mathbf{z}_t, \mathbf{x} = \mathbf{x}_\theta(\mathbf{z}_t, t)) = \text{Cat}\left(\mathbf{z}_s; \frac{Q_{t|s}\mathbf{z}_t \odot Q_s^\top \mathbf{x}_\theta(\mathbf{z}_t, t)}{\mathbf{z}_t^\top Q_t^\top \mathbf{x}_\theta(\mathbf{z}_t, t)}\right). \quad (16)$$

where $\mathbf{x}_\theta(\mathbf{z}_t, t): \mathcal{V} \times [0, 1] \rightarrow \Delta^K$ is an approximation for \mathbf{x} .

A.2 Absorbing state

For the absorbing state diffusion process we have $\boldsymbol{\pi} = \mathbf{m}$.

A.2.1 $q(\mathbf{z}_s|\mathbf{z}_t, \mathbf{x})$

Since, $\mathbf{z}_t \in \{\mathbf{x}, \mathbf{m}\}$, takes only 2 values we consider the separate cases: $\mathbf{z}_t = \mathbf{x}$ and $\mathbf{z}_t = \mathbf{m}$.

Case 1. Consider the case $\mathbf{z}_t = \mathbf{x}$ i.e. \mathbf{z}_t is unmasked. From (15), we have the following:

$$\begin{aligned} & q(\mathbf{z}_s|\mathbf{z}_t = \mathbf{x}, \mathbf{x}) \\ &= \text{Cat}\left(\mathbf{z}_s; \frac{[\alpha_{t|s}\mathbf{x} + (1-\alpha_{t|s})\mathbf{1}]\mathbf{m}^\top \mathbf{x} \odot [\alpha_s\mathbf{x} + (1-\alpha_s)\mathbf{m}]}{\alpha_t\mathbf{x}^\top \mathbf{x} + (1-\alpha_t)\mathbf{x}^\top \mathbf{m}}\right) \\ &= \text{Cat}\left(\mathbf{z}_s; \frac{[\alpha_{t|s}\mathbf{x}] \odot [\alpha_s\mathbf{x} + (1-\alpha_s)\mathbf{m}]}{\alpha_t}\right) \quad \because \mathbf{x}^\top \mathbf{m} = 0 \\ &= \text{Cat}\left(\mathbf{z}_s; \frac{\alpha_t \mathbf{x}}{\alpha_t}\right) \quad \because \mathbf{x}^\top \mathbf{m} = 0 \text{ and } \alpha_t = \alpha_{t|s}\alpha_s \\ &= \text{Cat}(\mathbf{z}_s; \mathbf{x}) \quad \because \alpha_t = \alpha_{t|s}\alpha_s \end{aligned} \quad (17)$$

Thus, we have the following:

$$q(\mathbf{z}_s|\mathbf{z}_t = \mathbf{x}, \mathbf{x}) = \text{Cat}(\mathbf{z}_s; \mathbf{x}). \quad (18)$$

Case 2. Consider the case $\mathbf{z}_t = \mathbf{m}$. By substituting $\mathbf{z}_t = \mathbf{m}$ and $\boldsymbol{\pi} = \mathbf{m}$ in (15), $q(\mathbf{z}_s|\mathbf{z}_t, \mathbf{x})$ simplifies to the following:

$$\begin{aligned} q(\mathbf{z}_s|\mathbf{z}_t = \mathbf{m}, \mathbf{x}) &= \text{Cat}\left(\mathbf{z}_s; \frac{(\alpha_{t|s}\mathbf{m} + (1-\alpha_{t|s})\mathbf{1}) \odot (\alpha_s\mathbf{x} + (1-\alpha_s)\mathbf{m})}{(1-\alpha_t)}\right) \\ &= \text{Cat}\left(\mathbf{z}_s; \frac{(\alpha_{t|s}(1-\alpha_s)\mathbf{m} + (1-\alpha_{t|s})(1-\alpha_s)\mathbf{m} + (\alpha_s - \alpha_t)\mathbf{x})}{(1-\alpha_t)}\right) \\ &= \text{Cat}\left(\mathbf{z}_s; \frac{(1-\alpha_s)\mathbf{m} + (\alpha_s - \alpha_t)\mathbf{x}}{1-\alpha_t}\right) \end{aligned} \quad (19)$$

Note that the above categorical distribution is non-zero for $\mathbf{z}_s \in \{\mathbf{x}, \mathbf{m}\}$ and zero for every other value. The non-zero values are specified as follows:

$$q(\mathbf{z}_s = \mathbf{x}|\mathbf{z}_t = \mathbf{m}, \mathbf{x}) = \frac{\alpha_s - \alpha_t}{1 - \alpha_t} \quad (20)$$

$$q(\mathbf{z}_s = \mathbf{m}|\mathbf{z}_t = \mathbf{m}, \mathbf{x}) = \frac{1 - \alpha_s}{1 - \alpha_t} \quad (21)$$

Combining Cases 1 and 2, we get:

$$q(\mathbf{z}_s|\mathbf{z}_t, \mathbf{x}) = \begin{cases} \text{Cat}(\mathbf{z}_s; \mathbf{z}_t) & \mathbf{z}_t \neq \mathbf{m}, \\ \text{Cat}\left(\mathbf{z}_s; \frac{(1-\alpha_s)\mathbf{m} + (\alpha_s - \alpha_t)\mathbf{x}}{1-\alpha_t}\right) & \mathbf{z}_t = \mathbf{m}. \end{cases} \quad (22)$$

A.2.2 $p_\theta(\mathbf{z}_s|\mathbf{z}_t)$

For the absorbing state diffusion process with $\boldsymbol{\pi} = \mathbf{m}$, we want to simplify the (16). For this reason, we consider 2 cases: first, when $\mathbf{z}_t \neq \mathbf{m}$ (**case 1**), second, when $\mathbf{z}_t = \mathbf{m}$ (**case 2**).

Case 1. Consider the case when $\mathbf{z}_t \neq \mathbf{m}$. (16) simplifies to the following:

$$\begin{aligned}
p_\theta(\mathbf{z}_s | \mathbf{z}_t \neq \mathbf{m}) &= \text{Cat}\left(\mathbf{z}_s; \frac{Q_{t|s} \mathbf{z}_t \odot Q_s^\top \mathbf{x}_\theta(\mathbf{z}_t, t)}{\mathbf{z}_t^\top Q_t^\top \mathbf{x}_\theta(\mathbf{z}_t, t)}\right) \\
&= \text{Cat}\left(\mathbf{z}_s; \frac{Q_{t|s} \mathbf{z}_t \odot Q_s^\top \mathbf{x}_\theta(\mathbf{z}_t, t)}{[Q_t \mathbf{z}_t]^\top \mathbf{x}_\theta(\mathbf{z}_t, t)}\right) \\
&= \text{Cat}\left(\mathbf{z}_s; \frac{[\alpha_{t|s} \mathbf{z}_t] \odot [\alpha_s \mathbf{I}_n + (1 - \alpha_s) \mathbf{m} \mathbf{1}^\top] \mathbf{x}_\theta(\mathbf{z}_t, t)}{[\alpha_t \mathbf{z}_t]^\top \mathbf{x}_\theta(\mathbf{z}_t, t)}\right) \\
&= \text{Cat}\left(\mathbf{z}_s; \frac{[\alpha_{t|s} \mathbf{z}_t] \odot [\alpha_s \mathbf{x}_\theta(\mathbf{z}_t, t) + (1 - \alpha_s) \mathbf{m} \langle \mathbf{1}, \mathbf{x}_\theta(\mathbf{z}_t, t) \rangle]}{\alpha_t \langle \mathbf{z}_t, \mathbf{x}_\theta(\mathbf{z}_t, t) \rangle}\right) \\
&\text{since } \langle \mathbf{1}, \mathbf{x}_\theta(\mathbf{z}_t, t) \rangle = 1, \text{ we have the following:} \\
&= \text{Cat}\left(\mathbf{z}_s; \frac{[\alpha_{t|s} \mathbf{z}_t] \odot [\alpha_s \mathbf{x}_\theta(\mathbf{z}_t, t) + (1 - \alpha_s) \mathbf{m}]}{\alpha_t \langle \mathbf{z}_t, \mathbf{x}_\theta(\mathbf{z}_t, t) \rangle}\right) \\
&\text{since } \mathbf{z}_t \odot \mathbf{m} = \mathbf{0}, \text{ we have the following:} \\
&= \text{Cat}\left(\mathbf{z}_s; \frac{\alpha_t \mathbf{z}_t \odot \mathbf{x}_\theta(\mathbf{z}_t, t)}{\alpha_t \langle \mathbf{z}_t, \mathbf{x}_\theta(\mathbf{z}_t, t) \rangle}\right) \tag{23}
\end{aligned}$$

Case 2. Consider the case when $\mathbf{z}_t = \mathbf{m}$. (16) simplifies to the following:

$$\begin{aligned}
p_\theta(\mathbf{z}_s | \mathbf{z}_t = \mathbf{m}) &= \text{Cat}\left(\mathbf{z}_s; \frac{Q_{t|s} \mathbf{m} \odot Q_s^\top \mathbf{x}_\theta(\mathbf{z}_t, t)}{\mathbf{m}^\top Q_t^\top \mathbf{x}_\theta(\mathbf{z}_t, t)}\right) \\
&= \text{Cat}\left(\mathbf{z}_s; \frac{Q_{t|s} \mathbf{m} \odot Q_s^\top \mathbf{x}_\theta(\mathbf{z}_t, t)}{[Q_t^\top \mathbf{m}]^\top \mathbf{x}_\theta(\mathbf{z}_t, t)}\right) \\
&= \text{Cat}\left(\mathbf{z}_s; \frac{[\alpha_{t|s} \mathbf{m} + (1 - \alpha_{t|s}) \mathbf{1}] \odot [\alpha_s \mathbf{I}_n + (1 - \alpha_s) \mathbf{m} \mathbf{1}^\top] \mathbf{x}_\theta(\mathbf{z}_t, t)}{[\alpha_t \mathbf{m} + (1 - \alpha_t) \mathbf{1}]^\top \mathbf{x}_\theta(\mathbf{z}_t, t)}\right) \\
&= \text{Cat}\left(\mathbf{z}_s; \frac{[\alpha_{t|s} \mathbf{m} + (1 - \alpha_{t|s}) \mathbf{1}] \odot [\alpha_s \mathbf{x}_\theta(\mathbf{z}_t, t) + (1 - \alpha_s) \mathbf{m} \langle \mathbf{1}, \mathbf{x}_\theta(\mathbf{z}_t, t) \rangle]}{\alpha_t \langle \mathbf{m}, \mathbf{x}_\theta(\mathbf{z}_t, t) \rangle + (1 - \alpha_t) \langle \mathbf{1}, \mathbf{x}_\theta(\mathbf{z}_t, t) \rangle}\right) \\
&= \text{Cat}\left(\mathbf{z}_s; \frac{[\alpha_{t|s} \mathbf{m} + (1 - \alpha_{t|s}) \mathbf{1}] \odot [\alpha_s \mathbf{x}_\theta(\mathbf{z}_t, t) + (1 - \alpha_s) \mathbf{m}]}{\alpha_t \langle \mathbf{x}_\theta(\mathbf{z}_t, t), \mathbf{m} \rangle + (1 - \alpha_t)}\right) \\
&= \text{Cat}\left(\mathbf{z}_s; \frac{\alpha_t \mathbf{m} \odot \mathbf{x}_\theta(\mathbf{z}_t, t) + (\alpha_s - \alpha_t) \mathbf{x}_\theta(\mathbf{z}_t, t) + (1 - \alpha_s) \mathbf{m}}{\alpha_t \langle \mathbf{x}_\theta(\mathbf{z}_t, t), \mathbf{m} \rangle + (1 - \alpha_t)}\right) \tag{24}
\end{aligned}$$

Note that the above categorical distribution, we can obtain the values for $p_\theta(\mathbf{z}_s = \mathbf{x} | \mathbf{z}_t = \mathbf{m})$ and $p_\theta(\mathbf{z}_s = \mathbf{m} | \mathbf{z}_t = \mathbf{m})$ which are as follows:

$$p_\theta(\mathbf{z}_s = \mathbf{x} | \mathbf{z}_t = \mathbf{m}) = \frac{(\alpha_s - \alpha_t) \langle \mathbf{x}_\theta(\mathbf{z}_t, t), \mathbf{x} \rangle}{\alpha_t \langle \mathbf{x}_\theta(\mathbf{z}_t, t), \mathbf{m} \rangle + (1 - \alpha_t)} \tag{25}$$

$$p_\theta(\mathbf{z}_s = \mathbf{m} | \mathbf{z}_t = \mathbf{m}) = \frac{\alpha_s \langle \mathbf{x}_\theta(\mathbf{z}_t, t), \mathbf{m} \rangle + (1 - \alpha_s)}{\alpha_t \langle \mathbf{x}_\theta(\mathbf{z}_t, t), \mathbf{m} \rangle + (1 - \alpha_t)} \tag{26}$$

As a sanity check, we can verify that (25) reduces to (20), and (26) reduces to (21) if our denoising network can reconstruct \mathbf{x} perfectly, i.e., $\mathbf{x}_\theta(\mathbf{z}_t, t) = \mathbf{x}$.

Combining (23) and (24), we get the following expression for the reverse process parameterization:

$$p_\theta(\mathbf{z}_s | \mathbf{z}_t) = \begin{cases} \text{Cat}\left(\mathbf{z}_s; \frac{\alpha_t \mathbf{z}_t \odot \mathbf{x}_\theta(\mathbf{z}_t, t)}{\alpha_t \langle \mathbf{z}_t, \mathbf{x}_\theta(\mathbf{z}_t, t) \rangle}\right) & \mathbf{z}_t \neq \mathbf{m}, \\ \text{Cat}\left(\mathbf{z}_s; \frac{\alpha_t \mathbf{m} \odot \mathbf{x}_\theta(\mathbf{z}_t, t) + (\alpha_s - \alpha_t) \mathbf{x}_\theta(\mathbf{z}_t, t) + (1 - \alpha_s) \mathbf{m}}{\alpha_t \langle \mathbf{x}_\theta(\mathbf{z}_t, t), \mathbf{m} \rangle + (1 - \alpha_t)}\right) & \mathbf{z}_t = \mathbf{m}. \end{cases} \tag{27}$$

A.2.3 Diffusion Loss

For a given T , Let $\mathcal{L}_T = \mathbb{E}_{t \in \{1, \dots, T\}} \mathbb{E}_{q(\mathbf{z}_t | \mathbf{x})} T \text{DKL}(q(\mathbf{z}_s | \mathbf{z}_t, \mathbf{x}) \| p_\theta(\mathbf{z}_s | \mathbf{z}_t))$ denote the diffusion loss. We break down the computation of $\text{DKL}(q(\mathbf{z}_s | \mathbf{z}_t, \mathbf{x}) \| p_\theta(\mathbf{z}_s | \mathbf{z}_t))$ into 2 cases: $\mathbf{z}_t = \mathbf{x}$ (**case 1**) and $\mathbf{z}_t = \mathbf{m}$ (**case 2**).

Case 1. consider the case $\mathbf{z}_t = \mathbf{x}$. Let's simplify $D_{\text{KL}}(q(\mathbf{z}_s|\mathbf{z}_t = \mathbf{x}, \mathbf{x})||p_\theta(\mathbf{z}_s|\mathbf{z}_t = \mathbf{x}))$.

$$\begin{aligned}
& D_{\text{KL}}(q(\mathbf{z}_s|\mathbf{z}_t = \mathbf{x}, \mathbf{x})||p_\theta(\mathbf{z}_s|\mathbf{z}_t = \mathbf{x})) \\
&= \sum_{\mathbf{z}_s} q(\mathbf{z}_s|\mathbf{z}_t = \mathbf{x}, \mathbf{x}) \log \frac{q(\mathbf{z}_s|\mathbf{z}_t = \mathbf{x}, \mathbf{x})}{p_\theta(\mathbf{z}_s|\mathbf{z}_t = \mathbf{x})} \\
&= \log \frac{1}{p_\theta(\mathbf{z}_s = \mathbf{x}|\mathbf{z}_t = \mathbf{x})} \quad \because q(\mathbf{z}_s = \mathbf{x}|\mathbf{z}_t, \mathbf{x}) = 1 \text{ and } q(\mathbf{z}_s \neq \mathbf{x}|\mathbf{z}_t, \mathbf{x}) = 0 \\
&= \log 1 \quad \text{From (23)} \\
&= 0 \quad (28)
\end{aligned}$$

Case 2. Consider the case $\mathbf{z}_t = \mathbf{m}$. Let's simplify $D_{\text{KL}}(q(\mathbf{z}_s|\mathbf{z}_t = \mathbf{m}, \mathbf{x})||p_\theta(\mathbf{z}_s|\mathbf{z}_t = \mathbf{m}))$.

$$\begin{aligned}
& D_{\text{KL}}(q(\mathbf{z}_s|\mathbf{z}_t = \mathbf{m}, \mathbf{x})||p_\theta(\mathbf{z}_s|\mathbf{z}_t = \mathbf{m})) \\
&= \sum_{\mathbf{z}_s} q(\mathbf{z}_s|\mathbf{z}_t = \mathbf{m}, \mathbf{x}) \log \frac{q(\mathbf{z}_s|\mathbf{z}_t = \mathbf{m}, \mathbf{x})}{p_\theta(\mathbf{z}_s|\mathbf{z}_t = \mathbf{m})} \\
&= \sum_{\mathbf{z}_s \in \{\mathbf{x}, \mathbf{m}\}} q(\mathbf{z}_s|\mathbf{z}_t = \mathbf{m}, \mathbf{x}) \log \frac{q(\mathbf{z}_s|\mathbf{z}_t = \mathbf{m}, \mathbf{x})}{p_\theta(\mathbf{z}_s|\mathbf{z}_t = \mathbf{m})} \\
&= \underbrace{q(\mathbf{z}_s = \mathbf{x}|\mathbf{z}_t = \mathbf{m}, \mathbf{x}) \log \frac{q(\mathbf{z}_s = \mathbf{x}|\mathbf{z}_t = \mathbf{m}, \mathbf{x})}{p_\theta(\mathbf{z}_s = \mathbf{x}|\mathbf{z}_t = \mathbf{m})}}_{\text{Simplify using (20) and (25)}} \\
&\quad + \underbrace{q(\mathbf{z}_s = \mathbf{m}|\mathbf{z}_t = \mathbf{m}, \mathbf{x}) \log \frac{q(\mathbf{z}_s = \mathbf{m}|\mathbf{z}_t = \mathbf{m}, \mathbf{x})}{p_\theta(\mathbf{z}_s = \mathbf{m}|\mathbf{z}_t = \mathbf{m})}}_{\text{Simplify using (21) and (26)}} \\
&= \frac{\alpha_s - \alpha_t}{1 - \alpha_t} \log \frac{\alpha_t \langle \mathbf{x}_\theta(\mathbf{z}_t, t), \mathbf{m} \rangle + (1 - \alpha_t)}{(1 - \alpha_t) \langle \mathbf{x}_\theta(\mathbf{z}_t, t), \mathbf{x} \rangle} \\
&\quad + \frac{1 - \alpha_s}{1 - \alpha_t} \log \frac{(1 - \alpha_s) (\alpha_t \langle \mathbf{x}_\theta(\mathbf{z}_t, t), \mathbf{m} \rangle + (1 - \alpha_t))}{(1 - \alpha_t) (\alpha_s \langle \mathbf{x}_\theta(\mathbf{z}_t, t), \mathbf{m} \rangle + (1 - \alpha_s))} \quad (29)
\end{aligned}$$

Thus, $D_{\text{KL}}(q(\mathbf{z}_s|\mathbf{z}_t, \mathbf{x})||p_\theta(\mathbf{z}_s|\mathbf{z}_t))$ can be written in the following manner where $\langle \mathbf{z}_t, \mathbf{x}_0 \rangle$ evaluates to 1 if $\mathbf{z}_t = \mathbf{x}$ and $\langle \mathbf{z}_t, \mathbf{m} \rangle$ evaluates to 1 if $\mathbf{z}_t = \mathbf{m}$:

$$\begin{aligned}
& D_{\text{KL}}(q(\mathbf{z}_s|\mathbf{z}_t, \mathbf{x})||p_\theta(\mathbf{z}_s|\mathbf{z}_t)) \\
&= \underbrace{D_{\text{KL}}(q(\mathbf{z}_s|\mathbf{z}_t = \mathbf{x}, \mathbf{x})||p_\theta(\mathbf{z}_s|\mathbf{z}_t = \mathbf{x}))}_{=0, \text{ from (28)}} \langle \mathbf{z}_t, \mathbf{x}_0 \rangle + \underbrace{D_{\text{KL}}(q(\mathbf{z}_s|\mathbf{z}_t = \mathbf{m}, \mathbf{x})||p_\theta(\mathbf{z}_s|\mathbf{z}_t = \mathbf{m}))}_{\text{Given by (29)}} \langle \mathbf{z}_t, \mathbf{m} \rangle \quad (30)
\end{aligned}$$

Thus, we derive the diffusion loss, \mathcal{L}_T , in the following manner:

$$\begin{aligned}
\mathcal{L}_T &= \mathbb{E}_{t \in \{\frac{1}{T}, \frac{2}{T}, \dots, 1\}} \mathbb{E}_{q(\mathbf{z}_t|\mathbf{x})} T D_{\text{KL}}(q(\mathbf{z}_s|\mathbf{z}_t, \mathbf{x})||p_\theta(\mathbf{z}_s|\mathbf{z}_t)) \\
&= \mathbb{E}_{t \in \{\frac{1}{T}, \frac{2}{T}, \dots, 1\}} \mathbb{E}_{q(\mathbf{z}_t|\mathbf{x})} T \left[\frac{\alpha_s - \alpha_t}{1 - \alpha_t} \log \frac{\alpha_t \langle \mathbf{x}_\theta(\mathbf{z}_t, t), \mathbf{m} \rangle + (1 - \alpha_t)}{(1 - \alpha_t) \langle \mathbf{x}_\theta(\mathbf{z}_t, t), \mathbf{x} \rangle} \right. \\
&\quad \left. + \frac{1 - \alpha_s}{1 - \alpha_t} \log \frac{(1 - \alpha_s) (\alpha_t \langle \mathbf{x}_\theta(\mathbf{z}_t, t), \mathbf{m} \rangle + (1 - \alpha_t))}{(1 - \alpha_t) (\alpha_s \langle \mathbf{x}_\theta(\mathbf{z}_t, t), \mathbf{m} \rangle + (1 - \alpha_s))} \right] \langle \mathbf{z}_t, \mathbf{m} \rangle \quad (31)
\end{aligned}$$

Note that \mathcal{L}_T is 0 if \mathbf{z}_t is an unmasked token i.e. $\mathbf{z}_t = \mathbf{x}$.

A.2.4 NELBO

Austin et al. [1], Sohl-Dickstein et al. [39] given latents $\mathbf{x}_{1, \dots, T}$, model α_i as $(\alpha_i)_{i \in \{1, \dots, T\}} = 1 - \frac{i}{T}$. However, in this paper, we denote the latents as $\mathbf{z}_{t(0), \dots, t(T)}$; and hence, the $\alpha_{t(i)}$ are given as follows:

$$(\alpha_i)_{i \in \{1, \dots, T\}} = 1 - \frac{i}{T} \quad \text{From Austin et al. [1], Sohl-Dickstein et al. [39].}$$

$$\begin{aligned}
&\implies (\alpha_i)_{k \in \{1, \dots, T+1\}} = 1 - \frac{i}{T+1} && \text{For } T+1 \text{ latents} \\
&\implies (\alpha_i)_{i \in \{0, \dots, T\}} = 1 - \frac{i+1}{T+1} && \text{Offsetting the indices by 1.} \\
&\implies (\alpha_{t(i)})_{i \in \{0, \dots, T\}} = 1 - \frac{i+1}{T+1} && \text{Switching the notations from } \alpha_i \text{ to } \alpha_{t(i)}. \quad (32)
\end{aligned}$$

Consequently, from Equation 32, we derive that

$$\alpha_{t(0)} = \frac{T}{T+1}, \quad (33)$$

$$\alpha_{t(T)} = 0. \quad (34)$$

Thus we have the following:

$$\mathbf{z}_{t(0)} \sim \text{Cat}(\cdot; \alpha_{t=0} \mathbf{x} + (1 - \alpha_{t=0}) \mathbf{m}) = \text{Cat}\left(\cdot; \frac{T}{T+1} \mathbf{x} + \frac{1}{T+1} \mathbf{m}\right), \quad (35)$$

$$q(\mathbf{z}_{t(T)} | \mathbf{x}) = \text{Cat}(\cdot; \alpha_{t=1} \mathbf{x} + (1 - \alpha_{t=1}) \mathbf{m}) = \text{Cat}(\cdot; \mathbf{m}), \quad (36)$$

$$p_\theta(\mathbf{z}_{t(T)}) = \text{Cat}(\cdot; \mathbf{m}) \quad (37)$$

The NELBO (2) simplifies to the following:

$$\begin{aligned}
&\mathbb{E}_q \left[-\log p_\theta(\mathbf{x} | \mathbf{z}_{t(0)}) + \underbrace{\mathcal{L}_T}_{\text{Compute using (31)}} \right] + \underbrace{D_{\text{KL}}[q(\mathbf{z}_{t(T)} | \mathbf{x}) \| p_\theta(\mathbf{z}_{t(T)})]}_{=0 \text{ using (36) and (37)}} \\
&= \mathbb{E}_{q,t} \left[-\log p_\theta(\mathbf{x} | \mathbf{z}_{t(0)}) + T \left[\frac{\alpha_s - \alpha_t}{1 - \alpha_t} \log \frac{\alpha_t \langle \mathbf{x}_\theta(\mathbf{z}_t, t), \mathbf{m} \rangle + (1 - \alpha_t)}{(1 - \alpha_t) \langle \mathbf{x}_\theta(\mathbf{z}_t, t), \mathbf{x} \rangle} \right. \right. \\
&\quad \left. \left. + \frac{1 - \alpha_s}{1 - \alpha_t} \log \frac{(1 - \alpha_s) (\alpha_t \langle \mathbf{x}_\theta(\mathbf{z}_t, t), \mathbf{m} \rangle + (1 - \alpha_t))}{(1 - \alpha_t) (\alpha_s \langle \mathbf{x}_\theta(\mathbf{z}_t, t), \mathbf{m} \rangle + (1 - \alpha_s))} \right] \langle \mathbf{z}_t, \mathbf{m} \rangle \right] \quad (38)
\end{aligned}$$

Appendix B MDLM

In this section we show how SUBS parameterization can simplify the functional form of the NELBO as defined in (38).

B.1 Rao-Blackwellization

We employ the RB techniques as described in Sec. 3.2.3 to simplify the NELBO (38) to (40) using RB2, and further to (42) using RB1.

B.1.1 Zero Masking Probabilities

Using ‘‘Zero Masking Probabilities’’ (RB2) from Sec. 3.2.3, we set $\langle \mathbf{x}_\theta(\mathbf{z}_t, t), \mathbf{m} \rangle = 0$ in (31) to obtain the following simplified diffusion loss:

$$\begin{aligned}
\mathcal{L}_T^{\text{RB2}} &= \mathbb{E}_{t \in \{1, \dots, T\}} \mathbb{E}_{q(\mathbf{z}_t | \mathbf{x})} T \left[\frac{\alpha_s - \alpha_t}{1 - \alpha_t} \log \frac{1}{\langle \mathbf{x}_\theta(\mathbf{z}_t, t), \mathbf{x} \rangle} \right] \langle \mathbf{z}_t, \mathbf{m} \rangle \\
&= \mathbb{E}_{t \in \{1, \dots, T\}} \mathbb{E}_{q(\mathbf{z}_t | \mathbf{x})} T \left[\frac{\alpha_t - \alpha_s}{1 - \alpha_t} \log \langle \mathbf{x}_\theta(\mathbf{z}_t, t), \mathbf{x} \rangle \right] \langle \mathbf{z}_t, \mathbf{m} \rangle. \quad (39)
\end{aligned}$$

The corresponding Rao-Blackwellized NELBO is given as:

$$\begin{aligned}
&\mathbb{E}_q \left[-\log p_\theta(\mathbf{x} | \mathbf{z}_{t(0)}) + \underbrace{\mathcal{L}_T^{\text{RB2}}}_{\text{Compute using (39)}} \right] + \underbrace{D_{\text{KL}}[q(\mathbf{z}_{t(T)} | \mathbf{x}) \| p_\theta(\mathbf{z}_{t(T)})]}_{=0 \text{ using (36) and (37)}} \\
&= \mathbb{E}_{q,t} \left[-\log p_\theta(\mathbf{x} | \mathbf{z}_{t(0)}) + T \left[\frac{\alpha_t - \alpha_s}{1 - \alpha_t} \log \langle \mathbf{x}_\theta(\mathbf{z}_t, t), \mathbf{x} \rangle \right] \langle \mathbf{z}_t, \mathbf{m} \rangle \right] \quad (40)
\end{aligned}$$

B.1.2 Carry Over Unmasking

Notice that the term $\langle \mathbf{x}_\theta(\mathbf{z}_t, t), \mathbf{m} \rangle$ in (39), reduces the diffusion loss to 0 for $\mathbf{z}_t \neq \mathbf{m}$ i.e. $\mathbf{z}_t = \mathbf{x}$. Now, we'd like to show that with ‘‘Carry Over Unmasking’’ (RB1) from Sec. 3.2.3, we can drop $\langle \mathbf{x}_\theta(\mathbf{z}_t, t), \mathbf{m} \rangle$ from (39). Recall that RB1 ensures $\mathbf{x}_\theta(\mathbf{z}_t, t) = \mathbf{x}$ for $\mathbf{z}_t = \mathbf{x}$. Thus, with RB1 parameterization the diffusion loss (39) reduces to 0 for $\mathbf{z}_t = \mathbf{x}$ since $\log \langle \mathbf{x}_\theta(\mathbf{z}_t, t), \mathbf{m} \rangle = 0$. This allows us to drop $\langle \mathbf{x}_\theta(\mathbf{z}_t, t), \mathbf{m} \rangle$ in (40) to obtain the following diffusion loss:

$$\mathcal{L}_T^{\text{RB2}+\text{RB1}} = \mathbb{E}_{t \in \{\frac{1}{T}, \frac{2}{T}, \dots, 1\}} \mathbb{E}_{q(\mathbf{z}_t | \mathbf{x})} T \left[\frac{\alpha_t - \alpha_s}{1 - \alpha_t} \log \langle \mathbf{x}_\theta(\mathbf{z}_t, t), \mathbf{x} \rangle \right] \quad (41)$$

B.1.3 NELBO

Thus, we have the following NELBO:

$$\begin{aligned} & \mathbb{E}_q \left[-\log p_\theta(\mathbf{x} | \mathbf{z}_{t(0)}) + \underbrace{\mathcal{L}_T^{\text{RB2}+\text{RB1}}}_{\text{Compute using (41)}} \right] + \underbrace{D_{\text{KL}}[q(\mathbf{z}_{t(T)} | \mathbf{x}) \| p_\theta(\mathbf{z}_{t(T)})]}_{= 0 \text{ using (36) and (37)}} \\ &= \mathbb{E}_{q,t} \left[-\log p_\theta(\mathbf{x} | \mathbf{z}_{t(0)}) + T \left[\frac{\alpha_t - \alpha_s}{1 - \alpha_t} \log \langle \mathbf{x}_\theta(\mathbf{z}_t, t), \mathbf{x} \rangle \right] \right] \end{aligned} \quad (42)$$

Comparing (42) and (40). Note that due to RB1, $\log p_\theta(\mathbf{x} | \mathbf{z}_{t(0)})$ in (42) reduces to 0 every time $\mathbf{z}_{t(0)} = \mathbf{x}$ as explained in (44). However, this is not the case in (40), even though it has a functionally similar expression to (42). Because of this reason (42) should lead to a better likelihood estimate and we empirically verify this in Table 8.

B.2 Continous Time

B.2.1 Diffusion Loss

To derive the continuous-time diffusion loss, $\mathcal{L}_{\text{diffusion}}^\infty$, we consider the limiting case $\lim_{T \rightarrow \infty} \mathcal{L}_T^{\text{RB2}+\text{RB1}}$ (41):

$$\begin{aligned} \mathcal{L}_{\text{diffusion}}^\infty &= \lim_{T \rightarrow \infty} \mathcal{L}_T^{\text{RB2}+\text{RB1}} \\ &= \mathbb{E}_{t \in \{\frac{1}{T}, \frac{2}{T}, \dots, 1\}, q(\mathbf{z}_t | \mathbf{x})} \left[\lim_{T \rightarrow \infty} T \frac{\alpha_t - \alpha_s}{1 - \alpha_t} \log \langle \mathbf{x}_\theta(\mathbf{z}_t, t), \mathbf{x} \rangle \right] \\ &= \mathbb{E}_{t \sim \mathcal{U}[0,1], q(\mathbf{z}_t | \mathbf{x})} \left[\frac{\alpha'_t}{1 - \alpha_t} \log \langle \mathbf{x}_\theta(\mathbf{z}_t, t), \mathbf{x} \rangle \right] \quad \text{Using } \lim_{T \rightarrow \infty} T(\alpha_t - \alpha_s) = \alpha'_t \end{aligned} \quad (43)$$

B.2.2 Reconstruction Loss

For the continous time case, from (35), we have

$$\begin{aligned} \mathbf{z}_{t(0)} &\sim \lim_{T \rightarrow \infty} \text{Cat} \left(\cdot; \frac{T}{T+1} \mathbf{x} + \frac{1}{T+1} \mathbf{m} \right) \\ &\implies \mathbf{z}_{t(0)} \sim \text{Cat}(\cdot; \mathbf{x}) \\ &\implies \mathbf{z}_{t(0)} = \mathbf{x} \end{aligned} \quad (44)$$

Thus, the reconstruction loss reduces to 0 in the following manner:

$$\begin{aligned} \mathcal{L}_{\text{recons}} &= -\log p_\theta(\mathbf{x} | \mathbf{z}_{t(0)}) \\ &= -\log p_\theta(\mathbf{x} | \mathbf{z}_{t(0)} = \mathbf{x}) \quad \text{From (44)} \\ &= -\log \langle \mathbf{x}_\theta(\mathbf{x}, t(0)), \mathbf{x} \rangle \\ &= -\log \langle \mathbf{x}, \mathbf{x} \rangle \quad \text{Due to ‘‘copy over’’ } \mathbf{x}_\theta(\mathbf{x}, t(0)) = \mathbf{x} \\ &= 0. \end{aligned} \quad (45)$$

B.2.3 NELBO

Thus, we have the following NELBO:

$$\begin{aligned} & \mathbb{E}_q \left[\underbrace{-\log p_\theta(\mathbf{x}|\mathbf{z}_{t(0)})}_{= 0 \text{ from (45)}} + \underbrace{\mathcal{L}_{\text{diffusion}}^\infty}_{\text{Compute using (41)}} \right] + \underbrace{D_{\text{KL}}[q(\mathbf{z}_{t(T)}|\mathbf{x})||p_\theta(\mathbf{z}_{t(T)})]}_{= 0 \text{ using (36) and (37)}} \\ & = \mathbb{E}_{q,t} \left[\frac{\alpha'_t}{1-\alpha_t} \log \langle \mathbf{x}_\theta(\mathbf{z}_t, t), \mathbf{x} \rangle \right] \end{aligned} \tag{46}$$

Appendix C Experimental details

C.1 Likelihood Evaluation

We use a single monte-carlo estimate for t to evaluate the likelihood. The low discrepancy sampler (C.3) plays a key role in reducing the variance of the estimate as seen in Table 8.

C.2 Avg. Number of Tokens seen

Given `training_steps`, `batch_size`, `context_length`, the number of tokens seen by the AR model is given as:

$$\text{training_steps} \times \text{batch_size} \times \text{context_length}. \tag{47}$$

However, this expression doesn't hold for a diffusion model, since at each training step, a fraction of the input tokens are masked before being fed to the model. Let p_m be the probability of a token being masked at a timestep t . For the log-linear schedule in our experiments, $p_m = t$. Thus, the expected number of tokens seen by the diffusion model is:

$$\begin{aligned} & \mathbb{E}_{t \sim \mathcal{U}[0,1]} [\text{training_steps} \times \text{batch_size} \times \text{context_length} \times p_m] \\ & = \text{training_steps} \times \text{batch_size} \times \text{context_length} \times \mathbb{E}_{t \sim \mathcal{U}[0,1]} [p_m] \\ & = \text{training_steps} \times \text{batch_size} \times \text{context_length} \times \mathbb{E}_{t \sim \mathcal{U}[0,1]} [t] \quad \because p_m = t \\ & = \text{training_steps} \times \text{batch_size} \times \text{context_length} \times 0.5. \quad \because \mathbb{E}_{t \sim \mathcal{U}[0,1]} [t] = 0.5 \end{aligned} \tag{48}$$

LM1B. Following [1, 25, 19], we train MDLM for 1M training steps with a `batch_size` = 512, and a context length of 128. Like [25] we use a log-linear schedule and hence the number of tokens seen by our model is $\approx 33\text{B}$ (48). Similarly, MDLM trained for 10M steps, saw 327B tokens in expectation. The corresponding AR baseline was trained for 0.5M and 5M steps to ensure a similar number of tokens was seen.

OWT. We train SEDD and MDLM for 1M training steps with a `batch_size` = 512, `context_length` = 1024, and log-linear schedule. Hence, these models saw

C.3 Low discrepancy sampler

To reduce variance during training we use a low-discrepancy sampler, similar to that proposed in Kingma et al. [21]. Specifically, when processing a minibatch of N samples, instead of independently sampling N from a uniform distribution, we partition the unit interval and sample the time step for each sequence $i \in \{1, \dots, N\}$ from a different portion of the interval $t_i \sim U[\frac{i-1}{N}, \frac{i}{N}]$. This ensures that our sampled timesteps are more evenly spaced across the interval $[0,1]$, reducing the variance of the ELBO.

C.4 Language Modeling

For our forward noise process, we use a log-linear noise schedule similar to Lou et al. [25].

We detokenize the One Billion Words dataset following Lou et al. [25], whose code can be found [here](#)¹. We tokenize the One Billion Words dataset with the `bert-base-uncased` tokenizer, following He et al. [19]. We pad and truncate sequences to a length of 128.

¹<https://github.com/louaaron/Score-Entropy-Discrete-Diffusion/blob/main/data.py>

We tokenize OpenWebText with the GPT2 tokenizer. We do not pad or truncate sequences – we concatenate and wrap them to a length of 1,024. When wrapping, we add the eos token in-between concatenated. We additionally set the first and last token of every batch to be eos. Since OpenWebText does not have a validation split, we leave the last 100k docs as validation.

We parameterize our autoregressive baselines, SEDD, and MDLM with the transformer architecture from Lou et al. [25]. We use 12 layers, a hidden dimension of 768, 12 attention heads, and a timestep embedding of 128 when applicable. Word embeddings are not tied between the input and output.

We use the AdamW optimizer with a batch size of 512, constant learning rate warmup from 0 to a learning rate of $3e-4$ for 2,500 steps. We use a constant learning rate for 1M, 5M, or 10M steps on One Billion Words, and 1M steps for OpenWebText. We use a dropout rate of 0.1.

C.5 Zeroshot Likelihood

We evaluate zeroshot likelihoods by taking the models trained on OpenWebText and evaluating likelihoods on the validation splits of 7 datasets: Penn Tree Bank (PTB; Marcus et al. [28]), Wikitext [29], One Billion Word Language Model Benchmark (LM1B; Chelba et al. [5]), Lambada [31], AG News [51], and Scientific Papers (Pubmed and Arxiv subsets; Cohan et al. [7]). We detokenize the datasets following Lou et al. [25]. For the AG News and Scientific Papers (Pubmed and Arxiv), we apply both the Wikitext and One Billion Words detokenizers. Since the zeroshot datasets have different conventions for sequence segmentation, we wrap sequences to 1024 and do not add eos tokens in between sequences.

C.6 Representation Learning

Following Devlin et al. [10], we evaluate on all GLUE tasks [50], but exclude WNLI.

We pre-train a MosaicBERT model on C4 [36] for 70k steps, corresponding to 36B tokens. We pad and truncate the data to 128 tokens using the `bert-base-uncased` tokenizer.

MosaicBERT [33] has a similar architecture to `bert-base-uncased` and has 137M parameters, 12 layers, 12 attention heads, a hidden dimension of 768, an intermediate size of 3072, and ALiBi attention bias [34].

For pre-training, we use the following hyperparameters: A global batch size of 4096 with gradient accumulation, a learning rate of $5e-4$, linear decay to 0.02x of the learning rate with a warmup of 0.06x of the full training duration, and the decoupled AdamW optimizer with $1e-5$ weight decay and betas 0.9 and 0.98.

For diffusion fine-tuning we use AdamW with a warmup of 2,500 steps from a learning rate of 0 to $5e-5$, betas 0.95 and 0.999, and batch size 512. We train for 5k steps total, corresponding to 32M tokens.

For GLUE evaluation, we use the HuggingFace script found [here](#)². We use the default parameters for all datasets, except for a batch size of 16, which we found helped with smaller datasets. This includes the default of 3 epochs for all datasets and learning rate of $2e-5$.

C.7 Diffusion DNA Models

Dataset We pre-train the Caduceus MLM [38] on the HG38 human reference genome [8]. Following Schiff et al. [38], we use character- / base pair-level tokenization. The dataset is based on the splits used in Avsec et al. [3]: the training split comprises of 35 billion tokens covering the human genome. This consists of 34,021 segments extended to a maximum length of 1,048,576 (220 segments). We maintain a constant 2^{20} tokens per batch. For the Genomics Benchmark tasks, we use 5-fold cross-validation where we split the training set into 90/10 train/validation splits.

Architecture The Caduceus MLM uses as a backbone a bi-directional variant of the data-dependent SSM Mamba block proposed in Gu et al. [16]. This architecture is ideal as it contains inductive biases that preserve reverse complement (RC) equivariance, respecting the inherent symmetry of double-stranded DNA molecules [27, 38, 52].

²<https://github.com/huggingface/transformers/tree/main/examples/pytorch/text-classification>

Training details All models are pre-trained on 10B tokens (10K steps) and fine-tuned on a generative objective for an additional 50B tokens (50K steps). We use a global batch size of 1024 for a context length of 1024 tokens. Downstream task fine-tuning is performed for 16K steps (1B tokens).

For performing Caduceus MLM pre-training, we follow Schiff et al. [38] for the model size configuration, and hyperparameter selection. For pre-training, we use a fixed 15% mask rate as done in Devlin et al. [10]. Of the 'masked' tokens, 80% are replaced with [MASK], 10% are replaced with a random token from the vocabulary, and 10% are left unchanged.

For fine-tuning all Mamba-based models (including Caduceus) on diffusion objectives, we lower the learning rate from 8e-3 to 1e-3. For fine-tuning HyenaDNA [30], we lower the learning rate from 6e-4 to 5e-5. Similar to Gu et al. [16], Schiff et al. [38], we found that Mamba-based models were robust to higher learning rates. We exclude timestep embeddings for all Diffusion DNA experiments, as we show it has minimal impact on generative performance (see Table 12, Suppl. D.5).

We perform downstream task fine-tuning on the final hidden state embedding from pre-training. We perform mean pooling across the sequence length, which may vary from 200 to approximately 2,000 bps. We report the mean and \pm on max/min classification accuracy over 5-fold cross-validation (CV) using different random seeds, with early stopping on validation accuracy. For each task, we do a hyperparameter sweep over batch size and learning rate and report the values of the 5-fold CV for the best configuration.

Genomic Benchmark Task Distributions We use a subset of the Genomic Benchmark tasks with an emphasis on tasks from Human data. The positive samples for each dataset were generated by selecting samples that were annotated, either computationally or experimentally, in previous work (e.g enhancers, promoters, open chromatin regions (OCR)) [14]. These annotations each correspond to subsets of the genome of varying sizes that may exhibit different distributions of DNA than those observed globally over the reference genome. Due to this, the observed dataset may have a different distribution than the data used for pre-training and calculating perplexity. This might in turn lead to a case where perplexity and downstream performance may not necessarily correlate.

Appendix D Additional Experiments

D.1 Noise schedule parameterization

As described in Sec. 3.4, the ELBO is invariant to the functional form of α_t . To demonstrate this, we evaluate MDLM, initially trained using a log-linear schedule on OWT, by replacing the noise schedule with various other noise schedules as mentioned below. Following prior works [1, 25, 39], we parameterize $\alpha_t = e^{-\sigma(t)}$, where $\sigma(t) : [0,1] \rightarrow \mathbb{R}^+$. Various functional forms of $\sigma(t)$ are listed below:

Log Linear [1, 25, 39]. The log linear schedule is given as:

$$\sigma(t) = -\log(1-t) \tag{49}$$

Cosine Squared schedule [18]. The Cosine Squared schedule is given as:

$$\sigma(t) = -\log \cos^2\left(\frac{\pi}{2}(1-t)\right) \tag{50}$$

Cosine schedule. The Cosine schedule is given as:

$$\sigma(t) = -\log \cos\left(\frac{\pi}{2}(1-t)\right) \tag{51}$$

Linear. The Linear schedule is given as:

$$\sigma(t) = \sigma_{\max} t \tag{52}$$

where σ_{\max} is a very large number. In our experiments we set it to 10^8 .

D.1.1 ELBO Invariance

The function α_t is invertible due to the monotonicity assumption in Sec. 3.1, and so we can perform the following change of variables in (10): $\gamma \equiv \log(1 - \alpha_t)$. Let $f : [0,1] \rightarrow \mathbb{R}^-$ be a function such

that $\gamma = f(t)$. Note that α_t goes through a monotonic transformation to obtain γ ; hence, γ is also monotonic in t since α_t is monotonic in t . This implies that the function f is invertible. Let $t = f^{-1}(\gamma)$. Then, we can we have the following diffusion loss:

$$\begin{aligned}
\mathcal{L}_{\text{NELBO}}^\infty &= \mathbb{E}_q \int_{t=0}^{t=1} \frac{\alpha'_t}{1-\alpha_t} \log \langle \mathbf{x}_\theta(\mathbf{z}_t, t), \mathbf{x} \rangle dt \\
&= -\mathbb{E}_q \int_{t=0}^{t=1} \log \langle \mathbf{x}_\theta(\mathbf{z}_t, t), \mathbf{x} \rangle \frac{d}{dt} [\log(1-\alpha_t)] dt \\
&= -\mathbb{E}_q \int_{t=0}^{t=1} \log \langle \mathbf{x}_\theta(\mathbf{z}_t, t), \mathbf{x} \rangle \frac{d}{dt} [f(t)] dt && \text{Substituting } f(t) = \log(1-\alpha_t) \\
&= -\mathbb{E}_q \int_{\gamma=-\infty}^{\gamma=0} \log \langle \mathbf{x}_\theta(\mathbf{z}_{f^{-1}(\gamma)}, f^{-1}(\gamma)), \mathbf{x} \rangle d\gamma && \text{Change of variables } \gamma \equiv f(t) \\
&= -\mathbb{E}_q \int_{\gamma=-\infty}^{\gamma=0} \log \langle \mathbf{x}_\theta(\tilde{\mathbf{z}}_\gamma, f^{-1}(\gamma)), \mathbf{x} \rangle d\gamma && \tilde{\mathbf{z}}_\gamma \equiv \mathbf{z}_{f^{-1}(\gamma)} \\
&= -\mathbb{E}_q \int_{\gamma=-\infty}^{\gamma=0} \log \langle \tilde{\mathbf{x}}_\theta(\tilde{\mathbf{z}}_\gamma, \gamma), \mathbf{x} \rangle d\gamma && \tilde{\mathbf{x}}_\theta(\tilde{\mathbf{z}}_\gamma, \gamma) \equiv \mathbf{x}_\theta(\tilde{\mathbf{z}}_\gamma, f^{-1}(\gamma)) \quad (53)
\end{aligned}$$

This new formulation demonstrates that the diffusion loss is invariant to the functional form of α_t . In Table 9 we demonstrate empirically that noise schedules with different functional forms evaluate to the same Likelihood which is consistent with our theory. However, different schedules lead to different per data point variance. Notably, the log-linear schedule exhibits the lowest variance among all the noise schedules considered.

Table 9: Likelihood in bits per dimension (BPD) for different noise schedules on OWT dataset, is reported along with the mean and variance associated with each noise schedule per data point. We empirically observe that noise schedules with different functional forms yield the same likelihood, consistent with our theory in Sec. 3.4; however, different schedules result in different variances.

$\sigma(t)$	Mean	Variance per datapoint
Log Linear (49)	3.30	1.81
Cosine (51)	3.30	3.30
Cosine Squared (50)	3.30	3.30
Linear (52)	3.30	7.57

D.2 Faster sampling with caching

In Figure 10 we compare the wall clock times of various methods: AR, SEDD, MDLM with caching, and MDLM without caching for generating 64 samples on a single GPU. When sampling in batches, a change of 1 token would necessitate a call to the denoising model. Therefore, smaller batch sizes have a lower likelihood of a token being unmasked. This might lead one to prefer generating samples in smaller batches, as opposed to using a larger batch size that fully saturates the GPU. Table 10 shows that generating samples with a batch size of 1 and using caching is twice as fast as generating samples without caching while fully utilizing the GPU. In Fig. 2, we observe that MDLM without caching yields samples that consistently get better generative perplexity than SEDD. For $T = \{5k, 10k\}$, both SEDD and MDLM get better generative perplexity than the AR model.

Table 10: Wall clock time reported in minutes to generate 64 samples on a single A5000 GPU.

	$T = 5k(\downarrow)$	$T = 10k(\downarrow)$
MDLM	70.3	127.9
+ caching	40.1	60.4

Generative perplexities across sample times on OpenWebText

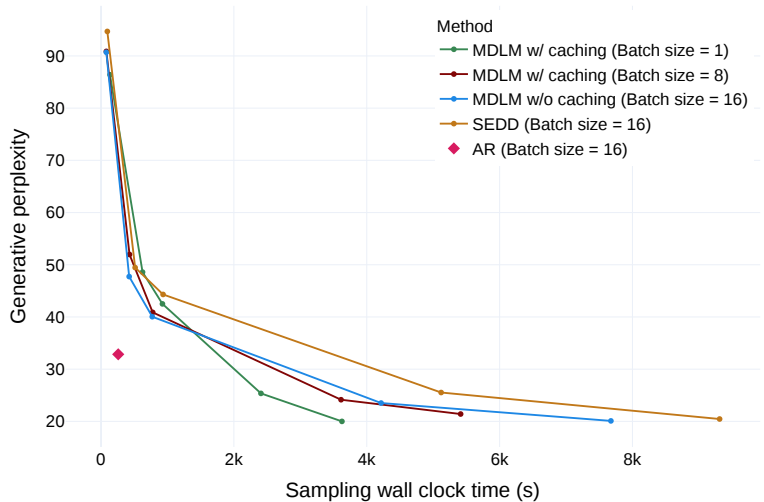


Figure 2: Generative perplexities across wall clock time for generating 64 samples on OWT using a single 32GB A5000 GPU are compared by varying $T \in \{100, 500, 1000, 5000, 10000\}$ in the reverse diffusion process. The samples are generated in mini-batches with a batch size of 16 for AR, SEDD, and MDLM without caching, as it is the largest batch size that fits on this GPU. For MDLM with caching, we vary the batch size.

D.3 LM1B ablations

We assess the importance of our continuous-time framework by performing ablation on diffusion steps T . In Table 11, we compare NLL and PPL under continuous and discrete T in MDLM. We find that NLL consistently decreases as $T \rightarrow \infty$.

Table 11: Discrete vs continuous time evaluation for MDLM w/o time-conditioning on OWT. MDLM was trained with $T = \infty$. We report test perplexity for a discrete T .

T	PPL(\leq)
∞	23.05
10	42.18
20	30.70
50	25.77
100	24.35
200	23.66
500	23.26
1000	23.15

D.4 Train NLL curves on OWT

In Figure 3, we show that MDLM achieves lower variance loss during training compared to a previous diffusion language model, SEDD. Training is performed over 1M steps on OWT (which corresponds to 524B tokens).



Figure 3: Train negative log-likelihood (NLL) curves across 1M gradient steps (524B tokens) on OpenWebText [13]. NLL is logged every 1K steps without value smoothing.

D.5 Time-conditioning ablation on OWT

In Table 12, we assess the importance of time conditioning in MDLM on OWT. We observe that time-conditioning has minimal impact on perplexity. Training is performed over 1M steps on OWT (which corresponds to 524B tokens).

Table 12: Ablation on time-conditioning in MDLM on OWT.

Method	PPL
MDLM w/ time-conditioning	23.21
MDLM w/o time-conditioning	23.05

NeurIPS Paper Checklist

The checklist is designed to encourage best practices for responsible machine learning research, addressing issues of reproducibility, transparency, research ethics, and societal impact. Do not remove the checklist: **The papers not including the checklist will be desk rejected.** The checklist should follow the references and follow the (optional) supplemental material. The checklist does NOT count towards the page limit.

Please read the checklist guidelines carefully for information on how to answer these questions. For each question in the checklist:

- You should answer [Yes], [No], or [NA].
- [NA] means either that the question is Not Applicable for that particular paper or the relevant information is Not Available.
- Please provide a short (1–2 sentence) justification right after your answer (even for NA).

The checklist answers are an integral part of your paper submission. They are visible to the reviewers, area chairs, senior area chairs, and ethics reviewers. You will be asked to also include it (after eventual revisions) with the final version of your paper, and its final version will be published with the paper.

The reviewers of your paper will be asked to use the checklist as one of the factors in their evaluation. While "[Yes]" is generally preferable to "[No]", it is perfectly acceptable to answer "[No]" provided a proper justification is given (e.g., "error bars are not reported because it would be too computationally expensive" or "we were unable to find the license for the dataset we used"). In general, answering "[No]" or "[NA]" is not grounds for rejection. While the questions are phrased in a binary way, we acknowledge that the true answer is often more nuanced, so please just use your best judgment and write a justification to elaborate. All supporting evidence can appear either in the main paper or the supplemental material, provided in appendix. If you answer [Yes] to a question, in the justification please point to the section(s) where related material for the question can be found.

IMPORTANT, please:

- **Delete this instruction block, but keep the section heading "NeurIPS paper checklist",**
- **Keep the checklist subsection headings, questions/answers and guidelines below.**
- **Do not modify the questions and only use the provided macros for your answers.**

1. Claims

Question: Do the main claims made in the abstract and introduction accurately reflect the paper's contributions and scope?

Answer: [Yes]

Justification: Claims are addressed

2. Limitations

Question: Does the paper discuss the limitations of the work performed by the authors?

Answer: [Yes]

Justification: Our method under-performs compared to autoregressive models. We also discuss other limitations in the paper.

3. Theory Assumptions and Proofs

Question: For each theoretical result, does the paper provide the full set of assumptions and a complete (and correct) proof?

Answer: [Yes]

Justification: They are in the proofs.

Guidelines:

- The answer NA means that the paper does not include theoretical results.

- All the theorems, formulas, and proofs in the paper should be numbered and cross-referenced.
- All assumptions should be clearly stated or referenced in the statement of any theorems.
- The proofs can either appear in the main paper or the supplemental material, but if they appear in the supplemental material, the authors are encouraged to provide a short proof sketch to provide intuition.
- Inversely, any informal proof provided in the core of the paper should be complemented by formal proofs provided in appendix or supplemental material.
- Theorems and Lemmas that the proof relies upon should be properly referenced.

4. Experimental Result Reproducibility

Question: Does the paper fully disclose all the information needed to reproduce the main experimental results of the paper to the extent that it affects the main claims and/or conclusions of the paper (regardless of whether the code and data are provided or not)?

Answer: [Yes]

Justification: We provide all hyperparameters necessary to reproduce the experiments and will provide code.

5. Open access to data and code

Question: Does the paper provide open access to the data and code, with sufficient instructions to faithfully reproduce the main experimental results, as described in supplemental material?

Answer: [No]

Justification: We will release all code after the paper is accepted. The datasets are already public.

Guidelines:

- The answer NA means that paper does not include experiments requiring code.
- Please see the NeurIPS code and data submission guidelines (<https://nips.cc/public/guides/CodeSubmissionPolicy>) for more details.
- While we encourage the release of code and data, we understand that this might not be possible, so “No” is an acceptable answer. Papers cannot be rejected simply for not including code, unless this is central to the contribution (e.g., for a new open-source benchmark).
- The instructions should contain the exact command and environment needed to run to reproduce the results. See the NeurIPS code and data submission guidelines (<https://nips.cc/public/guides/CodeSubmissionPolicy>) for more details.
- The authors should provide instructions on data access and preparation, including how to access the raw data, preprocessed data, intermediate data, and generated data, etc.
- The authors should provide scripts to reproduce all experimental results for the new proposed method and baselines. If only a subset of experiments are reproducible, they should state which ones are omitted from the script and why.
- At submission time, to preserve anonymity, the authors should release anonymized versions (if applicable).
- Providing as much information as possible in supplemental material (appended to the paper) is recommended, but including URLs to data and code is permitted.

6. Experimental Setting/Details

Question: Does the paper specify all the training and test details (e.g., data splits, hyperparameters, how they were chosen, type of optimizer, etc.) necessary to understand the results?

Answer: [Yes]

Justification: We provide detailed hyperparameters for all experiments.

Guidelines:

- The answer NA means that the paper does not include experiments.
- The experimental setting should be presented in the core of the paper to a level of detail that is necessary to appreciate the results and make sense of them.

- The full details can be provided either with the code, in appendix, or as supplemental material.

7. Experiment Statistical Significance

Question: Does the paper report error bars suitably and correctly defined or other appropriate information about the statistical significance of the experiments?

Answer: [Yes]

Justification: Many of our tables include error bars and standard deviations

Guidelines:

- The answer NA means that the paper does not include experiments.
- The authors should answer "Yes" if the results are accompanied by error bars, confidence intervals, or statistical significance tests, at least for the experiments that support the main claims of the paper.
- The factors of variability that the error bars are capturing should be clearly stated (for example, train/test split, initialization, random drawing of some parameter, or overall run with given experimental conditions).
- The method for calculating the error bars should be explained (closed form formula, call to a library function, bootstrap, etc.)
- The assumptions made should be given (e.g., Normally distributed errors).
- It should be clear whether the error bar is the standard deviation or the standard error of the mean.
- It is OK to report 1-sigma error bars, but one should state it. The authors should preferably report a 2-sigma error bar than state that they have a 96% CI, if the hypothesis of Normality of errors is not verified.
- For asymmetric distributions, the authors should be careful not to show in tables or figures symmetric error bars that would yield results that are out of range (e.g. negative error rates).

8. Experiments Compute Resources

Question: For each experiment, does the paper provide sufficient information on the computer resources (type of compute workers, memory, time of execution) needed to reproduce the experiments?

Answer: [Yes] .

Justification: We conduct all experiments on 8x 3090s, 8xA6000s, 8xA100s, or 8xH100s. The largest models on OpenWebText take 2 weeks to train on 8xA100, the LM1B models only take 2 days to train on the same hardware

Guidelines:

- The answer NA means that the paper does not include experiments.
- The paper should indicate the type of compute workers CPU or GPU, internal cluster, or cloud provider, including relevant memory and storage.
- The paper should provide the amount of compute required for each of the individual experimental runs as well as estimate the total compute.
- The paper should disclose whether the full research project required more compute than the experiments reported in the paper (e.g., preliminary or failed experiments that didn't make it into the paper).

9. Code Of Ethics

Question: Does the research conducted in the paper conform, in every respect, with the NeurIPS Code of Ethics <https://neurips.cc/public/EthicsGuidelines>?

Answer: [Yes]

Justification: We follow standard practices

Guidelines:

- The answer NA means that the authors have not reviewed the NeurIPS Code of Ethics.

- If the authors answer No, they should explain the special circumstances that require a deviation from the Code of Ethics.
- The authors should make sure to preserve anonymity (e.g., if there is a special consideration due to laws or regulations in their jurisdiction).

10. Broader Impacts

Question: Does the paper discuss both potential positive societal impacts and negative societal impacts of the work performed?

Answer: [Yes]

Justification: Our model will allow for more controllable text generation models, and do not increase the capability of current autoregressive models

Guidelines:

- The answer NA means that there is no societal impact of the work performed.
- If the authors answer NA or No, they should explain why their work has no societal impact or why the paper does not address societal impact.
- Examples of negative societal impacts include potential malicious or unintended uses (e.g., disinformation, generating fake profiles, surveillance), fairness considerations (e.g., deployment of technologies that could make decisions that unfairly impact specific groups), privacy considerations, and security considerations.
- The conference expects that many papers will be foundational research and not tied to particular applications, let alone deployments. However, if there is a direct path to any negative applications, the authors should point it out. For example, it is legitimate to point out that an improvement in the quality of generative models could be used to generate deepfakes for disinformation. On the other hand, it is not needed to point out that a generic algorithm for optimizing neural networks could enable people to train models that generate Deepfakes faster.
- The authors should consider possible harms that could arise when the technology is being used as intended and functioning correctly, harms that could arise when the technology is being used as intended but gives incorrect results, and harms following from (intentional or unintentional) misuse of the technology.
- If there are negative societal impacts, the authors could also discuss possible mitigation strategies (e.g., gated release of models, providing defenses in addition to attacks, mechanisms for monitoring misuse, mechanisms to monitor how a system learns from feedback over time, improving the efficiency and accessibility of ML).

11. Safeguards

Question: Does the paper describe safeguards that have been put in place for responsible release of data or models that have a high risk for misuse (e.g., pre-trained language models, image generators, or scraped datasets)?

Answer: [Yes]

Justification: These models are trained on trivial datasets and unlikely to cause any harm compared to state of the art language models.

Guidelines:

- The answer NA means that the paper poses no such risks.
- Released models that have a high risk for misuse or dual-use should be released with necessary safeguards to allow for controlled use of the model, for example by requiring that users adhere to usage guidelines or restrictions to access the model or implementing safety filters.
- Datasets that have been scraped from the Internet could pose safety risks. The authors should describe how they avoided releasing unsafe images.
- We recognize that providing effective safeguards is challenging, and many papers do not require this, but we encourage authors to take this into account and make a best faith effort.

12. Licenses for existing assets

Question: Are the creators or original owners of assets (e.g., code, data, models), used in the paper, properly credited and are the license and terms of use explicitly mentioned and properly respected?

Answer: [Yes]

Justification: All assets are publically available and we respect the licenses for all the data.

Guidelines:

- The answer NA means that the paper does not use existing assets.
- The authors should cite the original paper that produced the code package or dataset.
- The authors should state which version of the asset is used and, if possible, include a URL.
- The name of the license (e.g., CC-BY 4.0) should be included for each asset.
- For scraped data from a particular source (e.g., website), the copyright and terms of service of that source should be provided.
- If assets are released, the license, copyright information, and terms of use in the package should be provided. For popular datasets, paperswithcode.com/datasets has curated licenses for some datasets. Their licensing guide can help determine the license of a dataset.
- For existing datasets that are re-packaged, both the original license and the license of the derived asset (if it has changed) should be provided.
- If this information is not available online, the authors are encouraged to reach out to the asset's creators.

13. New Assets

Question: Are new assets introduced in the paper well documented and is the documentation provided alongside the assets?

Answer: [NA]

Justification: We provide no new assets.

Guidelines:

- The answer NA means that the paper does not release new assets.
- Researchers should communicate the details of the dataset/code/model as part of their submissions via structured templates. This includes details about training, license, limitations, etc.
- The paper should discuss whether and how consent was obtained from people whose asset is used.
- At submission time, remember to anonymize your assets (if applicable). You can either create an anonymized URL or include an anonymized zip file.

14. Crowdsourcing and Research with Human Subjects

Question: For crowdsourcing experiments and research with human subjects, does the paper include the full text of instructions given to participants and screenshots, if applicable, as well as details about compensation (if any)?

Answer: [NA]

Justification: [NA]

Guidelines:

- The answer NA means that the paper does not involve crowdsourcing nor research with human subjects.
- Including this information in the supplemental material is fine, but if the main contribution of the paper involves human subjects, then as much detail as possible should be included in the main paper.
- According to the NeurIPS Code of Ethics, workers involved in data collection, curation, or other labor should be paid at least the minimum wage in the country of the data collector.

15. Institutional Review Board (IRB) Approvals or Equivalent for Research with Human Subjects

Question: Does the paper describe potential risks incurred by study participants, whether such risks were disclosed to the subjects, and whether Institutional Review Board (IRB) approvals (or an equivalent approval/review based on the requirements of your country or institution) were obtained?

Answer: [NA]

Justification: [NA]

Guidelines:

- The answer NA means that the paper does not involve crowdsourcing nor research with human subjects.
- Depending on the country in which research is conducted, IRB approval (or equivalent) may be required for any human subjects research. If you obtained IRB approval, you should clearly state this in the paper.
- We recognize that the procedures for this may vary significantly between institutions and locations, and we expect authors to adhere to the NeurIPS Code of Ethics and the guidelines for their institution.
- For initial submissions, do not include any information that would break anonymity (if applicable), such as the institution conducting the review.